MULTIPLE TRELLIS-CODED MODULATION SCHEMES BASED ON TWO-DIMENSIONAL SIGNAL SETS FOR THE RAYLEIGH FADING CHANNEL

by

André Nadeau

58

A Thesis
Presented to the Faculty of Graduate Studies
in Partial Fulfillment of the Requirements
for the Degree

MASTER OF SCIENCE

Department of Electrical & Computer Engineering
University of Manitoba
Winnipeg, Manitoba

ISBN 0-612-13394-X

Canada

Name ANDRE NADEAU

Dissertation Abstracts International is arranged by broad, general subject categories. Please select the one subject which most nearly describes the content of your dissertation. Enter the corresponding four-digit code in the spaces provided.

ELECTRONICS AND ELECTRICAL

SUBJECT TERM

0544 U·M·I

SUBJECT CODE

Subject Categories

THE HUMANITIES AND SOCIAL SCIENCES

COMMUNICATIONS AND THE ARTS

Architecture 0729
Art History 0377
Cinema 0900
Dance 0378
Fine Arts 0357
Information Science 0723
Journalism 0391
Library Science 0399
Mass Communications 0708
Music 0413
Speech Communication 0459
Theater 0465

EDUCATION

General 0515
Administration 0514
Adult and Continuing 0516
Agricultural 0517
Art 0273
Bilingual and Multicultural 0282
Business 0688
Community College 0275
Curriculum and Instruction 0727
Early Childhood 0518
Elementary 0524
Finance 0277
Guidance and Counseling 0519
Health 0680
Higher 0745
History of 0520
Home Economics 0278
Industrial 0521
Language and Literature 0279
Mathematics 0280
Music 0522
Philosophy of 0998
Physical 0523
Psychology 0525
Reading 0535
Religious 0527
Sciences 0714
Secondary 0533
Social Sciences 0534
Sociology of 0340
Special 0529
Teacher Training 0530
Technology 0710
Tests and Measurements 0288
Vocational 0747

LANGUAGE, LITERATURE AND LINGUISTICS

Language
- General 0679
- Ancient 0289
- Linguistics 0290
- Modern 0291

Literature
- General 0401
- Classical 0294
- Comparative 0295
- Medieval 0297
- Modern 0298
- African 0316
- American 0591
- Asian 0305
- Canadian (English) 0352
- Canadian (French) 0355
- English 0593
- Germanic 0311
- Latin American 0312
- Middle Eastern 0315
- Romance 0313
- Slavic and East European 0314

PHILOSOPHY, RELIGION AND THEOLOGY

Philosophy 0422
Religion
- General 0318
- Biblical Studies 0321
- Clergy 0319
- History of 0320
- Philosophy of 0322

Theology 0469

SOCIAL SCIENCES

American Studies 0323
Anthropology
- Archaeology 0324
- Cultural 0326
- Physical 0327

Business Administration
- General 0310
- Accounting 0272
- Banking 0770
- Management 0454
- Marketing 0338

Canadian Studies 0385
Economics
- General 0501
- Agricultural 0503
- Commerce-Business 0505
- Finance 0508
- History 0509
- Labor 0510
- Theory 0511

Folklore 0358
Geography 0366
Gerontology 0351
History
- General 0578
- Ancient 0579
- Medieval 0581
- Modern 0582
- Black 0328
- African 0331
- Asia, Australia and Oceania 0332
- Canadian 0334
- European 0335
- Latin American 0336
- Middle Eastern 0333
- United States 0337

History of Science 0585
Law 0398
Political Science
- General 0615
- International Law and Relations 0616
- Public Administration 0617

Recreation 0814
Social Work 0452
Sociology
- General 0626
- Criminology and Penology 0627
- Demography 0938
- Ethnic and Racial Studies 0631
- Individual and Family Studies 0628
- Industrial and Labor Relations 0629
- Public and Social Welfare 0630
- Social Structure and Development 0700
- Theory and Methods 0344

Transportation 0709
Urban and Regional Planning 0999
Women's Studies 0453

THE SCIENCES AND ENGINEERING

BIOLOGICAL SCIENCES

Agriculture
- General 0473
- Agronomy 0285
- Animal Culture and Nutrition 0475
- Animal Pathology 0476
- Food Science and Technology 0359
- Forestry and Wildlife 0478
- Plant Culture 0479
- Plant Pathology 0480
- Plant Physiology 0817
- Range Management 0777
- Wood Technology 0746

Biology
- General 0306
- Anatomy 0287
- Biostatistics 0308
- Botany 0309
- Cell 0379
- Ecology 0329
- Entomology 0353
- Genetics 0369
- Limnology 0793
- Microbiology 0410
- Molecular 0307
- Neuroscience 0317
- Oceanography 0416
- Physiology 0433
- Radiation 0821
- Veterinary Science 0778
- Zoology 0472

Biophysics
- General 0786
- Medical 0760

EARTH SCIENCES

Biogeochemistry 0425
Geochemistry 0996
Geodesy 0370
Geology 0372
Geophysics 0373
Hydrology 0388
Mineralogy 0411
Paleobotany 0345
Paleoecology 0426
Paleontology 0418
Paleozoology 0985
Palynology 0427
Physical Geography 0368
Physical Oceanography 0415

HEALTH AND ENVIRONMENTAL SCIENCES

Environmental Sciences 0768
Health Sciences
- General 0566
- Audiology 0300
- Chemotherapy 0992
- Dentistry 0567
- Education 0350
- Hospital Management 0769
- Human Development 0758
- Immunology 0982
- Medicine and Surgery 0564
- Mental Health 0347
- Nursing 0569
- Nutrition 0570
- Obstetrics and Gynecology 0380
- Occupational Health and Therapy 0354
- Ophthalmology 0381
- Pathology 0571
- Pharmacology 0419
- Pharmacy 0572
- Physical Therapy 0382
- Public Health 0573
- Radiology 0574
- Recreation 0575
- Speech Pathology 0460
- Toxicology 0383

Home Economics 0386

PHYSICAL SCIENCES

Pure Sciences

Chemistry
- General 0485
- Agricultural 0749
- Analytical 0486
- Biochemistry 0487
- Inorganic 0488
- Nuclear 0738
- Organic 0490
- Pharmaceutical 0491
- Physical 0494
- Polymer 0495
- Radiation 0754

Mathematics 0405
Physics
- General 0605
- Acoustics 0986
- Astronomy and Astrophysics 0606
- Atmospheric Science 0608
- Atomic 0748
- Electronics and Electricity 0607
- Elementary Particles and High Energy 0798
- Fluid and Plasma 0759
- Molecular 0609
- Nuclear 0610
- Optics 0752
- Radiation 0756
- Solid State 0611

Statistics 0463

Applied Sciences

Applied Mechanics 0346
Computer Science 0984
Engineering
- General 0537
- Aerospace 0538
- Agricultural 0539
- Automotive 0540
- Biomedical 0541
- Chemical 0542
- Civil 0543
- Electronics and Electrical 0544
- Heat and Thermodynamics 0348
- Hydraulic 0545
- Industrial 0546
- Marine 0547
- Materials Science 0794
- Mechanical 0548
- Metallurgy 0743
- Mining 0551
- Nuclear 0552
- Packaging 0549
- Petroleum 0765
- Sanitary and Municipal 0554
- System Science 0790

Geotechnology 0428
Operations Research 0796
Plastics Technology 0795
Textile Technology 0994

PSYCHOLOGY

General 0621
Behavioral 0384
Clinical 0622
Developmental 0620
Experimental 0623
Industrial 0624
Personality 0625
Physiological 0989
Psychobiology 0349
Psychometrics 0632
Social 0451

Nom _____

Dissertation Abstracts International est organisé en catégories de sujets. Veuillez s.v.p. choisir le sujet qui décrit le mieux votre thèse et inscrivez le code numérique approprié dans l'espace réservé ci-dessous.

_____ ☐☐☐ U·M·I

SUJET — CODE DE SUJET

Catégories par sujets

HUMANITÉS ET SCIENCES SOCIALES

COMMUNICATIONS ET LES ARTS
Architecture 0729
Beaux-arts 0357
Bibliothéconomie 0399
Cinéma 0900
Communication verbale 0459
Communications 0708
Danse 0378
Histoire de l'art 0377
Journalisme 0391
Musique 0413
Sciences de l'information 0723
Théâtre 0465

ÉDUCATION
Généralités 515
Administration 0514
Art 0273
Collèges communautaires 0275
Commerce 0688
Économie domestique 0278
Éducation permanente 0516
Éducation préscolaire 0518
Éducation sanitaire 0680
Enseignement agricole 0517
Enseignement bilingue et multiculturel 0282
Enseignement industriel 0521
Enseignement primaire. 0524
Enseignement professionnel 0747
Enseignement religieux 0527
Enseignement secondaire 0533
Enseignement spécial 0529
Enseignement supérieur 0745
Évaluation 0288
Finances 0277
Formation des enseignants 0530
Histoire de l'éducation 0520
Langues et littérature 0279
Lecture 0535
Mathématiques 0280
Musique 0522
Orientation et consultation 0519
Philosophie de l'éducation 0998
Physique 0523
Programmes d'études et enseignement 0727
Psychologie 0525
Sciences 0714
Sciences sociales 0534
Sociologie de l'éducation 0340
Technologie 0710

LANGUE, LITTÉRATURE ET LINGUISTIQUE
Langues
- Généralités 0679
- Anciennes 0289
- Linguistique 0290
- Modernes 0291

Littérature
- Généralités 0401
- Anciennes 0294
- Comparée 0295
- Médiévale 0297
- Moderne 0298
- Africaine 0316
- Américaine 0591
- Anglaise 0593
- Asiatique 0305
- Canadienne (Anglaise) 0352
- Canadienne (Française) 0355
- Germanique 0311
- Latino-américaine 0312
- Moyen-orientale 0315
- Romane 0313
- Slave et est-européenne 0314

PHILOSOPHIE, RELIGION ET THÉOLOGIE
Philosophie 0422
Religion
- Généralités 0318
- Clergé 0319
- Études bibliques 0321
- Histoire des religions 0320
- Philosophie de la religion 0322

Théologie 0469

SCIENCES SOCIALES
Anthropologie
- Archéologie 0324
- Culturelle 0326
- Physique 0327

Droit 0398
Économie
- Généralités 0501
- Commerce-Affaires 0505
- Économie agricole 0503
- Économie du travail 0510
- Finances 0508
- Histoire 0509
- Théorie 0511

Études américaines 0323
Études canadiennes 0385
Études féministes 0453
Folklore 0358
Géographie 0366
Gérontologie 0351
Gestion des affaires
- Généralités 0310
- Administration 0454
- Banques 0770
- Comptabilité 0272
- Marketing 0338

Histoire
- Histoire générale 0578
- Ancienne 0579
- Médiévale 0581
- Moderne 0582
- Histoire des noirs 0328
- Africaine 0331
- Canadienne 0334
- États-Unis 0337
- Européenne 0335
- Moyen-orientale 0333
- Latino-américaine 0336
- Asie, Australie et Océanie 0332

Histoire des sciences 0585
Loisirs 0814
Planification urbaine et régionale 0999
Science politique
- Généralités 0615
- Administration publique 0617
- Droit et relations internationales 0616

Sociologie
- Généralités 0626
- Aide et bien-être social 0630
- Criminologie et établissements pénitentiaires 0627
- Démographie 0938
- Études de l' individu et de la famille 0628
- Études des relations interethniques et des relations raciales 0631
- Structure et développement social 0700
- Théorie et méthodes. 0344
- Travail et relations industrielles 0629

Transports 0709
Travail social 0452

SCIENCES ET INGÉNIERIE

SCIENCES BIOLOGIQUES
Agriculture
- Généralités 0473
- Agronomie. 0285
- Alimentation et technologie alimentaire 0359
- Culture 0479
- Élevage et alimentation 0475
- Exploitation des pâturages 0777
- Pathologie animale 0476
- Pathologie végétale 0480
- Physiologie végétale 0817
- Sylviculture et faune 0478
- Technologie du bois 0746

Biologie
- Généralités 0306
- Anatomie 0287
- Biologie (Statistiques) 0308
- Biologie moléculaire 0307
- Botanique 0309
- Cellule 0379
- Écologie 0329
- Entomologie 0353
- Génétique 0369
- Limnologie 0793
- Microbiologie 0410
- Neurologie 0317
- Océanographie 0416
- Physiologie 0433
- Radiation 0821
- Science vétérinaire 0778
- Zoologie 0472

Biophysique
- Généralités 0786
- Medicale 0760

SCIENCES DE LA TERRE
Biogéochimie 0425
Géochimie 0996
Géodésie 0370
Géographie physique 0368
Géologie 0372
Géophysique 0373
Hydrologie 0388
Minéralogie 0411
Océanographie physique 0415
Paléobotanique 0345
Paléoécologie 0426
Paléontologie 0418
Paléozoologie 0985
Palynologie 0427

SCIENCES DE LA SANTÉ ET DE L'ENVIRONNEMENT
Économie domestique 0386
Sciences de l'environnement 0768
Sciences de la santé
- Généralités 0566
- Administration des hôpitaux 0769
- Alimentation et nutrition 0570
- Audiologie 0300
- Chimiothérapie 0992
- Dentisterie 0567
- Développement humain 0758
- Enseignement 0350
- Immunologie 0982
- Loisirs 0575
- Médecine du travail et thérapie 0354
- Médecine et chirurgie 0564
- Obstétrique et gynécologie 0380
- Ophtalmologie 0381
- Orthophonie 0460
- Pathologie 0571
- Pharmacie 0572
- Pharmacologie 0419
- Physiothérapie 0382
- Radiologie 0574
- Santé mentale 0347
- Santé publique 0573
- Soins infirmiers 0569
- Toxicologie 0383

SCIENCES PHYSIQUES
Sciences Pures
Chimie
- Généralités 0485
- Biochimie 487
- Chimie agricole 0749
- Chimie analytique 0486
- Chimie minérale 0488
- Chimie nucléaire 0738
- Chimie organique 0490
- Chimie pharmaceutique 0491
- Physique 0494
- PolymÈres 0495
- Radiation 0754

Mathématiques 0405
Physique
- Généralités 0605
- Acoustique 0986
- Astronomie et astrophysique 0606
- Électronique et électricité 0607
- Fluides et plasma 0759
- Météorologie 0608
- Optique 0752
- Particules (Physique nucléaire) 0798
- Physique atomique 0748
- Physique de l'état solide 0611
- Physique moléculaire 0609
- Physique nucléaire 0610
- Radiation 0756

Statistiques 0463

Sciences Appliqués Et Technologie
Informatique 0984
Ingénierie
- Généralités 0537
- Agricole 0539
- Automobile 0540
- Biomédicale 0541
- Chaleur et thermodynamique 0348
- Conditionnement (Emballage) 0549
- Génie aérospatial 0538
- Génie chimique 0542
- Génie civil 0543
- Génie électronique et électrique 0544
- Génie industriel 0546
- Génie mécanique 0548
- Génie nucléaire 0552
- Ingénierie des systèmes 0790
- Mécanique navale 0547
- Métallurgie 0743
- Science des matériaux 0794
- Technique du pétrole 0765
- Technique minière 0551
- Techniques sanitaires et municipales 0554
- Technologie hydraulique 0545

Mécanique appliquée 0346
Géotechnologie 0428
Matières plastiques (Technologie) 0795
Recherche opérationnelle 0796
Textiles et tissus (Technologie) 0794

PSYCHOLOGIE
Généralités 0621
Personnalité 0625
Psychobiologie 0349
Psychologie clinique 0622
Psychologie du comportement 0384
Psychologie du développement 0620
Psychologie expérimentale 0623
Psychologie industrielle 0624
Psychologie physiologique 0989
Psychologie sociale 0451
Psychométrie 0632

MULTIPLE TRELLIS-CODED MODULATION SCHEMES BASED ON TWO-DIMENSIONAL SIGNAL SETS FOR THE RAYLEIGH FADING CHANNEL

BY

ANDRÉ NADEAU

A Thesis submitted to the Faculty of Graduate Studies of the University of Manitoba in partial fulfillment of the requirements for the degree of

MASTER OF SCIENCE

I hereby declare that I am the sole author of this thesis.

I authorize the University of Manitoba to lend this thesis to other institutions or individulals for the purpose of scholarly research.

Andre Nadeau

I further authorize the University of Manitoba to reproduce this thesis by photocopying or other means, in total or in part, at the request of other institutions or individuals for the purpose of scholarly research.

Andre Nadeau

ACKNOWLEDGEMENT

I am indebted to my advisor, Dr. Ed Shwedyk, for his insights and enduring patience. He always found time in his busy schedule to encourage me and to offer valuable suggestions for improvement.

I owe a particular debt of gratitude to the Canadian Forces and the Canadian People for providing the funds which have made my studies possible.

Finally, I acknowledge the understanding and support of my wife, Susan; she makes it all worthwhile.

ABSTRACT

This thesis designed and analyzed multiple trellis-coded modulation (MTCM) schemes based on multiple quadrature-amplitude modulation (M-QAM) and similar two-dimensional signal constellations for the Rayleigh fading channel. A method to partition two-dimensional signal sets for MTCM was first developed. This partitioning method was then used to partition 8- and 32-SQ as well as 8-, 16- and 64-QAM composite signal sets according to two criteria that ensured optimum partitioning for the Rayleigh fading channel. Next, a number of MTCM schemes based on these signal sets were designed and their error performance were analyzed. Finally, component diversity was combined with these MTCM schemes in order to increase their error performance.

Table of contents

List of figures and tables

Chapter 1 - Introduction

1.1 - Background

The mobile radio communication field is expanding rapidly with the introduction of a number of new systems such as cellular telephone and pager systems supported by land-based or satellite networks. Unfortunately, the allocation of bandwidth to mobile radio has not kept pace with the rapid increase of users [29,50]. In the United States, for example, the number of users has increased on average by 80-100% a year in recent years and this trend is predicted to continue for some time yet. As a result, some networks are fast becoming congested. The recent introduction of more efficient, fully digital systems to replace existing analogue networks has been helpful in slowing down this congestion but the problem still exists.

Considerable research is being conducted in all aspects of mobile radio communications to improve both the capacity and the performance of future all-digital mobile communication networks. Network control techniques such as multiple access have the potential to significantly increase the user base [1,30,34]. Unfortunately, these techniques are difficult to implement in many mobile radio communication contexts because of the rapidly changing morphology of networks as users enter and exit network cells. Data compression techniques can be very useful as demonstrated by Stern [51] and will likely be incorporated in future systems. Research in antenna design may also be helpful in increasing the capacity and performance of these mobile radio communication networks [5]. The introduction of more efficient modulation and coding schemes is yet another method by which improvements may be made.

The use of larger signal constellations to increase network capacity is a major trend in the development of modulation schemes for mobile communications [60]. However, loss in error performance is a major disadvantage of this approach. The use of error-correcting codes can offset the loss in performance but only at the cost of an

increase in transmission bandwidth or a lower information throughput. Trellis-Coded Modulation (TCM) and a variant, Multiple Trellis-Coded Modulation (MTCM), may be better suited to mobile radio communications because they provide considerable coding gains usually at no cost in transmission bandwidth, information throughput or power requirements.

The design of TCM schemes for mobile radio communications is limited currently to M-ary Amplitude Modulation (M-AM) and M-ary Phase Shift Keying (M-PSK) signal constellations. The performance of TCM and MTCM schemes based on these one-dimensional constellations decreases sharply with the number of symbols in the signal constellation[1]. Higher dimensional constellations such as two-dimensional M-ary Quadrature Amplitude Modulation (M-QAM) are better suited for large signal constellations. Unfortunately, the design of TCM and MTCM schemes based on M-QAM and similar two-dimensional constellations has proven to be a difficult task up to now.

It is useful to summarize the characteristics of the mobile radio channel as well as some of the assumptions made throughout this thesis. More thorough treatments of this topic are found in [7,32,36]. Figure 1.1 illustrates a typical mobile radio communication scenario. In this scenario, a mobile receiver in a vehicle receives a signal emitted by a fixed transmitter. The received signal consists of three components: the direct line-of-sight component, the specular reflection component and the diffuse component. The direct line of sight component is unaffected by reflection and propagates unimpeded from the transmitter and the receiver. The specular reflection component is that portion of the transmitted signal that is reflected to the receiver by a specular surface(s). This component differs from the direct line-of-sight component by a phase angle. The diffuse component is the sum of the multiple signals reflected by a multitude of non-specular

---

[1] The M-PSK constellation is two-dimensional in the cartesian coordinate system. However, the phase is the only coordinate that differentiates the symbols in the polar coordinate system since all symbols have the same amplitude. Therefore, the M-PSK constellation may be regarded as one-dimensional.

surfaces such as buildings and other vehicles. The envelope of the diffuse component exhibits a Rayleigh distribution while its phase is characterized by a uniform distribution. This fading is referred to as Rayleigh fading or multipath fading.

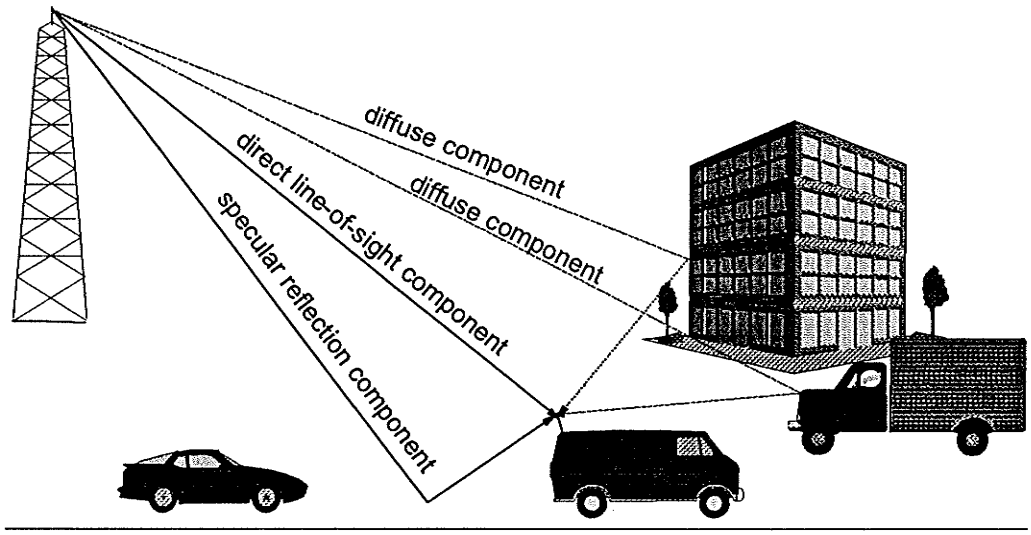

Figure 1.1 - Typical mobile radio communication scenario

In a typical mobile radio communication environment such as a typical urban center, measurements have shown that the direct-path and specular components are negligible most of the time [32]. When this occurs, the Rayleigh fading component dominates and the channel is at its poorest. In this thesis, the radio communication channel is assumed to be characterized solely by the diffuse component. This is a reasonable assumption since congested networks are almost always located in densely populated urban centres characterized by numerous large buildings and heavy traffic that encourage diffuse reflections.

The system block diagram for the mobile radio communication channel used throughout this thesis is illustrated in figure 1.2. The input bits are first encoded into symbols of the signal set by the trellis encoder. This process is later described in Chapter 2. The symbols are then interleaved. The combination of interleaving and de-interleaving has two purposes. First, it ensures that a series of consecutive symbols are not all

affected by a deep fade that lasts over many signalling intervals. Second, it allows one to assume that the fading coefficients over any signalling interval are uncorrelated to the fading coefficients over any other signalling interval. This assumption considerably simplifies the analyses on which this thesis is based. The symbols are then modulated and transmitted over the Rayleigh fading channel. It is assumed that the effect of the fading on the phase of the received signal is fully compensated for either by tracking it with some sort of phase-lock loop or with pilot tone calibration techniques [19]. The received symbols, corrupted by fading and Additive-White-Gaussian Noise (AWGN), are then demodulated and de-interleaved. Finally, the maximum-likelihood detection is performed through a Viterbi decoder.

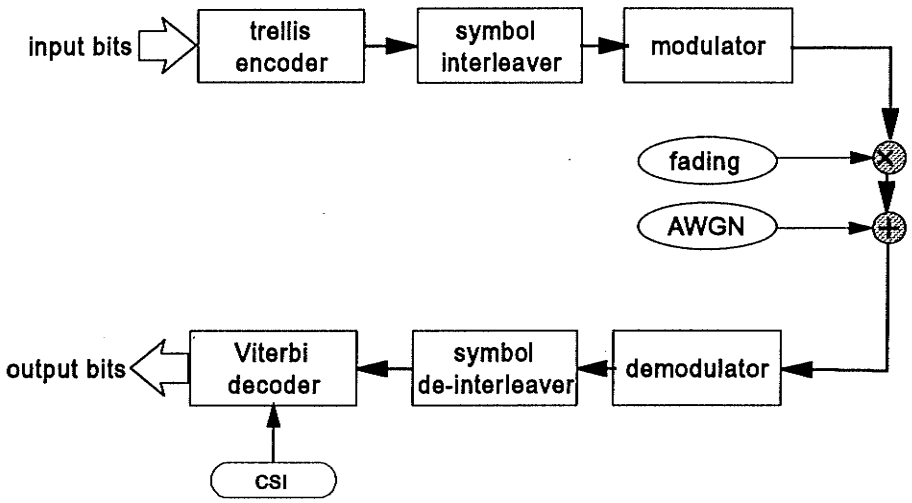

Figure 1.2 - System block diagram

This thesis assumes that channel-state information (CSI) in the form of fading coefficients for each signalling interval is available at the receiver. This last assumption is necessary because the error performance of two-dimensional constellations over the Rayleigh fading channel is irreducible if CSI is not available. The CSI may be obtained from channel sounding techniques such as the pilot tone-aided scheme [42] and pilot symbol-aided scheme [11,48,50].

1.2 - Aim and scope

The aim of this thesis is to design TCM and MTCM schemes based on M-QAM and similar two-dimensional signal constellations for mobile radio communications and analyse their performance. This thesis makes no attempt to develop a mobile communication system. The research is strictly limited to the search for TCM and MTCM schemes for mobile radio communications. There is no claim that the schemes developed herein can or will be applied in a practical system as the design of such a system involves the consideration of many factors, many of which conflict. However, the research conducted for this thesis can be readily adapted to the search for TCM and MTCM schemes that may be better suited for such an operational system.

Due to the nature of the material contained in this thesis, the reader would benefit from an understanding of basic communication theory and particularly of modulation techniques. There is a variety of reference material on these topics such as the textbook by Couch [15] and they are readily available. The reader would also benefit from a basic understanding of convolutional codes. This material can be found in textbooks by Blahut, and Lin/Costello [8,40].

1.3 - Outline

This thesis is organized in five chapters. Chapter 1 contains the introduction. Chapter 2 provides an overview of TCM and MTCM schemes for the AWGN channel. The importance of signal partitioning is highlighted and a technique to partition a two-dimensional signal set for MTCM is developed. Chapter 3 develops TCM and MTCM schemes based on M-QAM and other two-dimensional constellations for the Rayleigh fading channel. The performance of these schemes is measured and compared with the performance of equivalent M-PSK schemes. Chapter 4 describes the component diversity technique which can increase the performance of a communication system over the mobile radio communication channel and shows how the technique may be applied to

the MTCM schemes developed in Chapter 3. Chapter 5 summarizes the results of this thesis and suggests additional areas of research.

Chapter 2- TCM and MTCM for the AWGN channel

2.1 - General

This chapter briefly describes trellis-coded modulation (TCM) and multiple trellis-coded modulation (MTCM) techniques. Both techniques combine coding and modulation to improve the performance of digital transmission over band-limited channels. They yield significant coding gains over uncoded multilevel modulation without an increase in bandwidth or a decrease in the information throughput. Section 2.2 is a brief overview of TCM which is included as background material. Section 2.3 addresses MTCM. In particular, signal partitioning for MTCM is covered in section 2.3.2. A useful method to partition a two-dimensional signal set for MTCM is developed. This method will be used extensively in Chapter 3 to design MTCM schemes for the Rayleigh fading channel.

The material in this chapter assumes that the communication channel is non-dispersive and affected solely by AWGN. The criteria for designing trellis codes for the Rayleigh fading channel will be covered in Chapter 3. The criteria for designing trellis codes for other types of channels vary and are beyond the scope of this thesis. Readers who are interested in this information are referred to [35,43,46,52,62].

2.2 - Trellis-coded modulation

2.2.1 - Basic principles

The first TCM schemes were proposed by Ungerboeck in 1976 [56] followed by a more detailed publication in 1982 [55]. TCM has since been extensively researched and some applications have been developed. Most notably, a TCM scheme has now been adopted as the international standard for the coded 9.6-kbit/s two-wire full-duplex voiceband modem [7].

In conventional uncoded multilevel modulation, the transmitted bits are modulated into individual symbols of a signal set Ω and the noise-corrupted received signal is demodulated symbol by symbol. All received symbols are assumed to be statistically independent. The demodulation is conducted by comparing the squared Euclidean distance between the received symbols and each symbol of the signal set and by selecting the symbol that minimizes that distance. The minimum squared Euclidean distance is expressed as

$$d_{min}^2 = \min_{x_j \in \Omega} \|x - x_j\|^2$$

where x represents the received signals corrupted by AWGN and x_j represents the symbols in the signal set. The performance of the symbol-by-symbol receiver depends on the minimum squared Euclidean distance. The symbol error probability P[error] is upper-bounded [7] and, for large signal-to-noise ratio, closely approximated by

$$P[\text{error}] \leq \frac{M-1}{2} \text{erfc}\left(\frac{d_{min}}{2\sqrt{N_0}}\right)$$

where M is the number of symbols in the signal set, N_o is the white noise power spectral density and erfc(x) is given by

$$\text{erfc}(x) = \frac{2}{\sqrt{\pi}} \int_x^\infty e^{-t^2} dt$$

It is useful to define the normalized squared minimum distance δ^2,

$$\delta^2 = \frac{d_{min}^2}{E} \log_2 M$$

where E is the average energy of the signal set. Using this quantity, the upper bound for P[error] can be rewritten as

$$P[\text{error}] \leq \frac{M-1}{2}\operatorname{erfc}\left(\frac{\delta}{2}\sqrt{\frac{E_b}{N_0}}\right)$$

where E_b represents the average energy per bit and is given by $E_b = \frac{E}{\log_2 M}$. To design an efficient communication system, the minimum distance between any two symbols in a signal set must therefore be maximized for a given M and E_b.

TCM differs from conventional modulation by combining a convolutional encoder and an expanded signal set. Figure 2.1 shows a TCM transmitter. The information bits are encoded through a rate n/(n+r) convolutional encoder with memory ν. The expanded signal set is $2^{n+r}/2^n=2^r$ times as large as the signal set for the equivalent uncoded modulation. For r=1 as is the case throughout this thesis, the expanded signal set is twice as large as the original signal set.

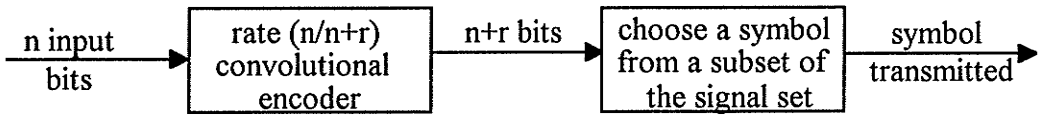

Figure 2.1 - TCM transmitter

One of the n+1 bits is used to select one of two subsets of a signal set Ω and the n remaining bits select one symbol from that subset. The particular subset chosen for a specific signalling interval depends on the state of the convolutional encoder at that time. The receiver recovers the original information bits by combining the demodulation and the decoding in a single process. In TCM, the transmitted symbols are no longer independent due to the use of the convolutional encoder but form a sequence $\mathbf{x}=(x_0, x_1, x_2, \ldots, x_N)$. The decoding is therefore conducted over a sequence $\hat{\mathbf{x}} = (\hat{x}_0, \hat{x}_1, \hat{x}_2, \ldots, \hat{x}_N)$.

In this case, the minimum distance d^2_{free} between two sequences is given by

$$d^2_{free} = \min_{\hat{x} \neq x} \left(\sum_{i=0}^{N} \left\| \hat{x}_i - x_i \right\|^2 \right)$$

that is, if the sequence $(x_0, x_1, ..., x_N)$ is closer to the received sequence than any other allowable symbol sequence. Because of the summation, d^2_{free} for efficient TCM schemes is larger than d^2_{min} for an equivalent uncoded modulation schemes. The error performance of TCM schemes is therefore superior to the error performance of equivalent uncoded modulation schemes.

A detailed explanation of TCM is beyond the scope of this thesis. However, the example in the next section should clarify its intricacies.

2.2.2 - Example of a TCM scheme

The following example of a rate 2/3 TCM scheme based on 8-PSK illustrates the salient points of TCM. First, the partitioning of the signal set is discussed. A diagram representation of the TCM scheme is then introduced, followed by an examination of the convolutional encoder. In isolation, each of these topics may be confusing. Accordingly, due to their interdependence, they should be studied together.

Signal partitioning refers to the decomposition of the signal set into subsets. The 8-PSK signal set Ω for the example is shown in Figure 2.2a. The signal set is partitioned into two subsets of four symbols each. These two subsets are further partitioned into four sub-subsets of two symbols each as shown: Sub-subset 1 is composed of symbols 0 and 4; sub-subset 2 is composed of symbols 2 and 6; sub-subset 3 is composed of symbols 1 and 5; andsSub-subset 4 is composed of signals 3 and 7. The composition of the sub-subsets is critical as it determines the performance of the TCM scheme. Signal partitioning will be examined in greater detail in section 2.2.3.

A trellis diagram for this example is depicted at Figure 2.2b. The trellis diagram provides a graphic representation of a TCM scheme. Although different terminology is

used by various authors, the following trellis diagram nomenclature is well accepted and used throughout this paper. A node represents one of the possible states of the convolutional encoder. Since there are only two nodes, the convolutional encoder for this TCM scheme has a memory of $\nu = 1$. The spacing between two nodes represents one signalling interval. A transition between two nodes is referred to as a branch. Each branch may be made up of more than one parallel path. The trellis at Figure 2.2b has two nodes with two branches per node. Each branch is made up of two parallel paths. Therefore, the trellis has a total of eight paths. Symbols from the signal set of Figure 2.2a are assigned to these paths. Since there are two input information bits, there must be 2^2=4 paths at each node of the trellis to ensure that all combinations of input bits are represented regardless of the state of the convolutional encoder during that particular signalling interval. The four symbols assigned to the four paths from the node at state 0 are 0, 4 ,2 and 6. Similarly, the four symbols assigned to the node at state 1 are 1, 5, 3 and 7.

Figure 2.2c illustrates an alternate representation of a trellis diagram. This representation is useful for the more complex trellises considered later in the thesis. The representation only shows one signalling interval since the trellis diagram for each successive signalling interval is the same. The number of parallel paths per branch is indicated over the slash through the first branch. The symbols assigned to the paths exiting a node are denoted to the left of the node. The leftmost two symbols are assigned to the two parallel paths of the uppermost branch exiting that node. The last two symbols are assigned to the two parallel paths of the next highest branch exiting the node. As Figure 2.2c shows, the two symbols assigned to the two parallel paths between two nodes at state 0 are symbols 0 and 4. The remainder of the representation is clarified by the following comparison of Figures 2.2b and 2.2c .

Figure 2.2d shows the convolutional encoder for the TCM scheme. The two input information bits are depicted as a_0 and a_1. Only a_1 is encoded through the rate 1/2 convolutional encoder with memory ν=1. Since the encoder has a memory of one, the state of the encoder can take 2^1=2 values, either zero or one. The encoded bit b_1 is used

to select one of the two subsets. The encoded bit b_2 is then used to select one of the two sub-subsets from that subset[2]. Finally, the bit $b_0=a_0$ is used to select one of the two symbols from the selected subset. Table 2.1 shows the relationship between the input information bits, the current state of the convolutional encoder and the symbol transmitted and illustrates the various combinations. For example, assume the convolutional encoder state is currently zero and that bits $a_0=0$ and $a_1=1$. From Table 2.1, we find that bits (b_1b_2) are (01) and select sub-subset 2. Bit $b_0=0$ selects the first symbol in that sub-subset, namely symbol 2. Furthermore, the new state of the convolutional encoder becomes 1. In the trellis, symbol 2 is assigned to the first branch of the transaction from the node representing state 0 (current state of the convolutional encoder) to the node representing state 1 (new state of the convolutional encoder). Similarly, symbol 7 is assigned to the second branch of the transaction from the node representing state 1 to the node representing state 0.

a_0 a_1	current encoder state	b_0 b_1 b_2	symbol selected	new encoder state
0 0	0	0 0 0	0	0
1 0	0	1 0 0	4	0
0 1	0	0 0 1	2	1
1 1	1	1 0 1	6	1
0 0	1	0 1 1	3	0
1 0	1	1 1 1	7	0
0 1	1	0 1 0	1	1
1 1	1	1 1 0	5	1

Table 2.1 - Relationship between the input information bits, the current state of the encoder and the symbol transmitted.

The distance properties of the above TCM scheme can be studied through its trellis diagram. The optimum decoding is the search for the path through the trellis that exhibits the minimum squared Euclidean distance once the received symbol sequence has been observed at the channel output. This search is best performed using the Viterbi algorithm

---

[2] This is equivalent to saying that the combination b_1b_2 selects one of the four sub-subsets.

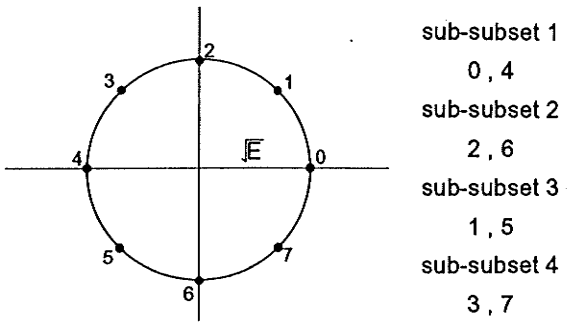

(a) - Subsets for 8-PSK signal set

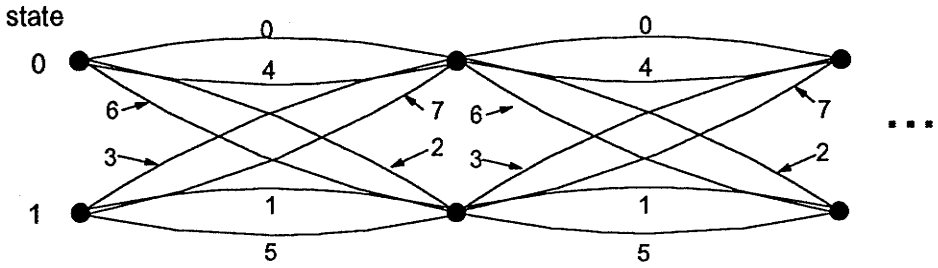

(b) - Trellis diagram representation

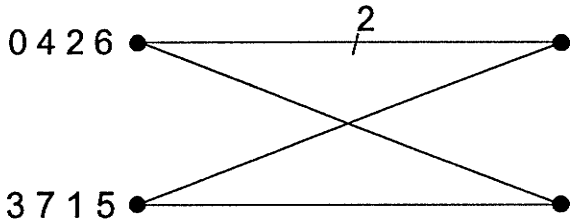

(c) - Alternative trellis representation

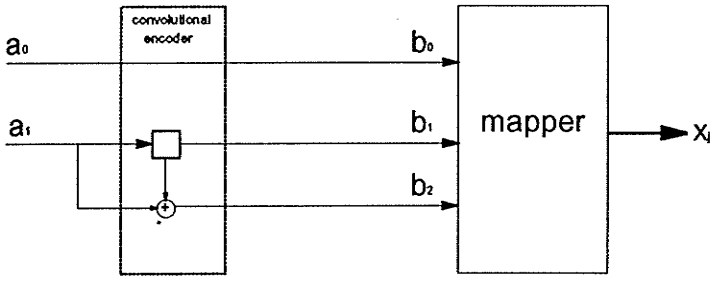

(d) - Convolutional encoder

Figure 2.2 - Rate 2/3 TCM scheme based on 8-PSK

[25,57]. Because of the noise in the channel, the received sequence may not coincide with the correct path (i.e., the sequence of transmitted symbols), but will occasionally diverge from it and re-emerge after a time L. When this occurs, one says that an error event of length L has occurred. The free distance of a TCM scheme is the minimum Euclidean distance between any pair of paths forming an error event.

In the above example, first consider an error event of length L=1. Consider state 0 in the trellis and assume that symbol 0 is transmitted but signal 4 is decoded. This is shown in Figure 2.3a. Since the transmitted symbols and the recovered symbols are different, an error has occurred. In this case, the path diverges and re-emerges at the same state (parallel paths) over a single signalling interval and therefore, L=1. The squared Euclidean distance for this error event is the squared Euclidean distance between symbols 0 and 4 which equals 4E. Next, consider the case represented at Figure 2.3b where the sequence of symbols 0,0 is transmitted and the sequence of symbols 2,7 is received. The error event is now of length L=2 and the Euclidean distance over the error event is

$$d^2_{L=2} = d^2(0,2) + d^2(0,7) = 2E + 4E\sin^2\frac{\pi}{8} = 2.586E$$

It is easy to show that no error events of length $L \geq 2$ yield a lower Euclidean distance than 2.56E. Therefore, the free distance of this code is d^2_{free}=2.56E.

The performance for this TCM scheme may be measured against uncoded 4-PSK (QPSK) modulation. This is a reasonable comparison because the information rate, the bandwidth and the average energy are the same for both modulation schemes. The asymptotic coding gain between two modulation schemes A and B is defined as

$$\gamma = \frac{d^2_{free/A}/E_A}{d^2_{free/B}/E_B}$$

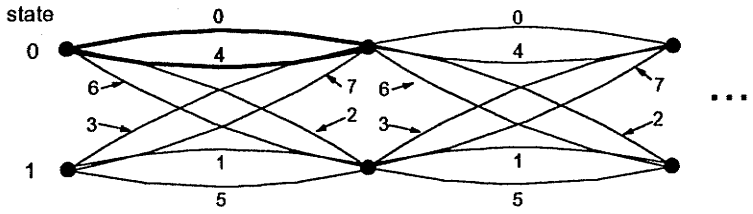

(a) - Error event over parallel paths

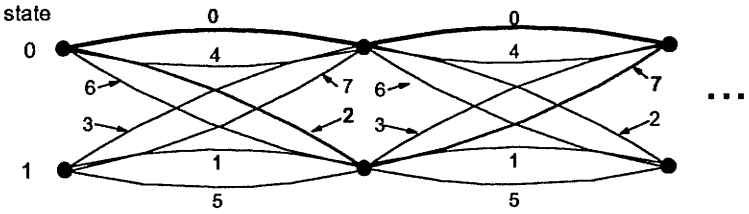

(b) - error event over two branches

Figure 2-3 - Error events for rate 2/3 TCM scheme based on 8-PSK

The asymptotic gain of this TCM scheme over uncoded QPSK is

$$\gamma = \frac{2.586/1}{2/1} = 1.293 \quad \Rightarrow \quad 1.1\,\text{dB}$$

The TCM scheme results in a symbol error performance gain of 1.1 dB over uncoded QPSK. This minor improvement in performance barely compensates for the related increase in complexity. However, greater improvements in error performance may be obtained by using more complex schemes involving larger numbers of states. For example, a scheme using the same signal set but with four states achieves a gain of 3.0 dB over uncoded QPSK. For an eight-state trellis, the gain improves to 3.6 dB. These figures represent significant performance gains.

2.2.3 - Signal partitioning and trellis mapping

It is apparent from the above example that the performance of a TCM scheme depends on how the symbols are mapped to the various paths in the trellis. Many

combinations are possible, some of which will actually lead to TCM schemes with poorer performance than uncoded QPSK. For an optimum scheme, the symbols must be assigned to the trellis paths so as to maximize d_{free}. In [55], Ungerboeck describes a simple procedure to partition one- or two-dimensional signal sets into subsets. He also develops three rules that facilitates the optimum mapping of these subsets onto various trellises. These topics are examined in this section.

Figure 2.4 represents the Ungerboeck partitioning of the 8-PSK signal set used in the previous example. The set partitioning is conducted in three stages. At the first level of partitioning (level 1), the eight symbols are divided into two subsets of four symbols each in such a way that the minimum squared Euclidean distance between the symbols in each subset is maximized. The process is repeated at the second level of partitioning (level 2). Each subset at the first level of partitioning is further partitioned into two 2-symbol subsets. Again, the minimum squared Euclidean distance between the two symbols in each subset at the second level of partitioning is maximized. At the third level of partitioning (level 3), each subset contains a single symbol. The above procedure guarantees that the minimum squared Euclidean distance between symbols in two subsets emanating from the same higher-level subset is greater than the minimum squared Euclidean distance between the symbols in two subsets at the same level of partitioning, but emanating from two different subsets at a higher level of partitioning.

Once the set partitioning is completed, the mapping of the subsets to the trellis may be conducted according to the three Ungerboeck rules. These rules are as follows:

U1. To parallel paths are assigned symbols of the same subset at the lowest level of partitioning where the number of symbols in each subset equals the number of parallel paths;

U2. To adjacent branches are assigned symbols of the next higher subsets; and

U3. All symbols are used equally often.

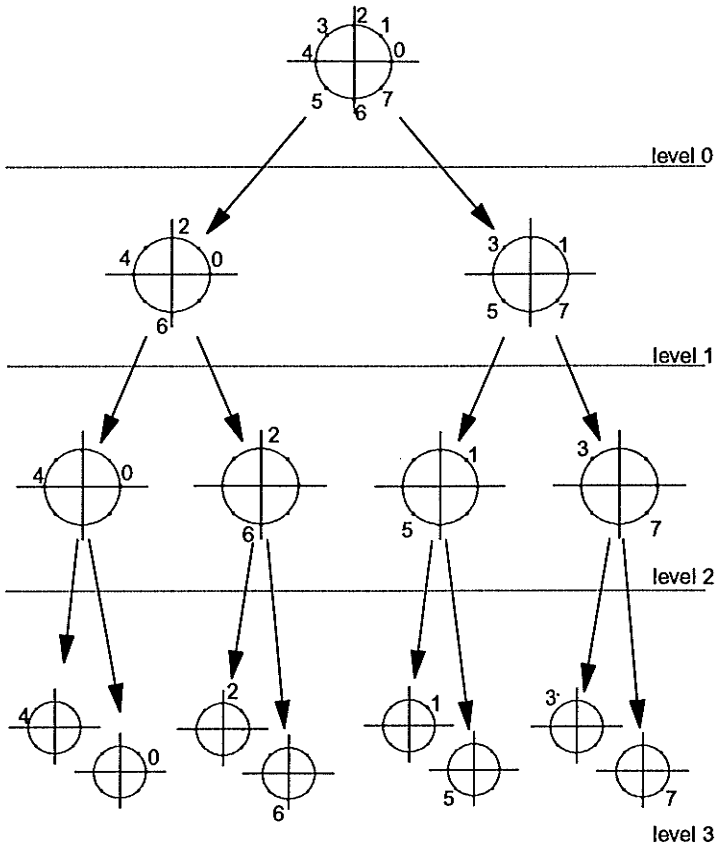

Figure 2.4 - Ungerboeck partitioning of 8-PSK

In order to design an optimum TCM scheme, the three Ungerboeck rules must be satisfied. However, satisfying these three rules does not ensure that a trellis is optimum. Many trellis codes satisfying these rules exist but only a small number of them are optimum. Unfortunately, a easy to follow step-by-step procedure to design optimum schemes does not exist. As a result, exhaustive computer searches are often the only viable solution to generate optimum schemes. The duration of computer searches increases exponentially with the number of states in a trellis and makes the design of trellis codes with large number of states often impractical.

The application of the three Ungerboeck rules is illustrated by reviewing the optimum trellis at Figure 2.2b. Consider the two parallel paths on the branch between two nodes at state 0. Note that the symbols 0 and 4 are assigned to the two parallel paths in the branch and that these two symbols are in the same subset at the second level of partitioning. Similarly, the two parallel paths in all other branches are assigned symbols from the same subsets at the second level of partitioning. These symbol assignments to parallel paths conform to rule U1. In a trellis without parallel paths, rule U1 can be ignored.

Rule U2 states that symbols from the next higher subset must be assigned to adjacent branches from a node. Since symbols 0 and 4 have been assigned to one branch of the node at state 0, symbols 2 and 6 must be assigned to the other branch since these four symbols are in the same subset at the first level of partitioning. Finally, the symbols 1,3,5 and 7 must be assigned to the branches at the nodes representing state 1 since rule U3 states that all symbols must be used equally often in the trellis.

2.2.4 - Convolutional encoder

A discussion on trellis codes would not be complete without considering the convolution encoder. The general structure of a TCM encoder/modulator is shown at Figure 2.5. There are n input information bits. A minimum signal set of 2^n symbols is required to transmit the 2^n combination of input bits. Of the n input bits, m are left uncoded. The remaining n-m bits are encoded by a convolutional encoder with rate (n-m)/(n-m+1). The n-m+1 encoded bits select a subset of the signal set and the m uncoded bits select a symbol within that subset. The memory of the convolutional encoder determines the number of states in the trellis. If all n bits are encoded, then the n+1 encoded bits select one symbol from the signal set and there are no parallel paths. In general, the specific structure of the convolutional encoder is not important. It is sufficient to state that such an encoder exists for a particular trellis code. For this reason, convolutional encoders need not be discussed further in this thesis.

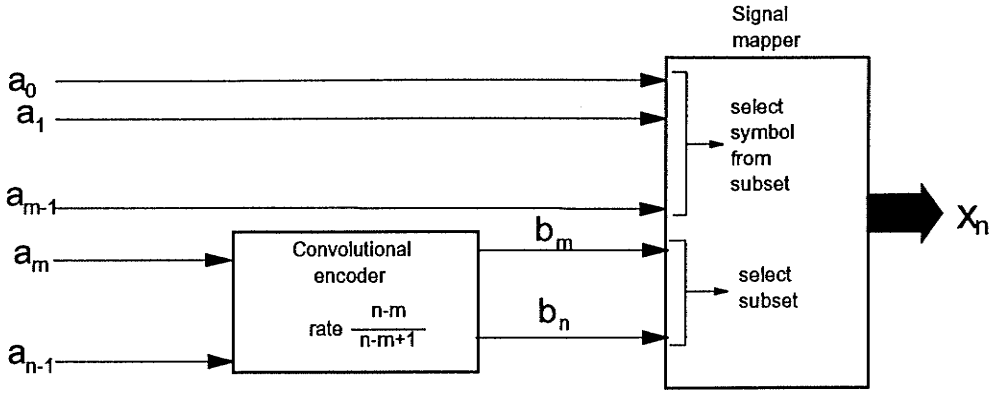

Figure 2.5 - TCM encoder/modulator

2.3 - Multiple trellis-coded modulation

2.3.1 - Basic principles

MTCM is a technique developed by Divsalar and Simon [18] to improve the free distance of trellis codes. That technique has proven to be especially useful for the Rayleigh fading channel. MTCM is a more general representation of trellis-coded modulation. MTCM combines a nk/(n+1)k convolutional encoder with a 2^{n+1}-point signal set to output k symbols in each signalling interval[3]. In each signalling interval, kn bits enter the encoder and k symbols leave the modulator. As a result, the bandwidth expansion relative to an uncoded 2^n-point signal constellation is unity. The parameter k is referred to as the multiplicity of the code.

Once again, it is useful to describe MTCM through an example. Consider the optimum 2-state, rate 4/6, k=2 MTCM scheme based on a 8-PSK signal set shown at Figure 2.6. The convolutional encoder inputs 4 information bits and outputs 6 coded bits in each signalling interval. Since the 4 information bits may represent 2^4=16 possible

[3] TCM is a special case of MTCM for which k=1.

combinations of input bits, there must be 8 parallel paths in each of the two branches exiting a trellis node. Each of these parallel paths is assigned two symbols from the 8-PSK signal set. We shall refer to the k symbols assigned to each path as the composite symbols for that path.

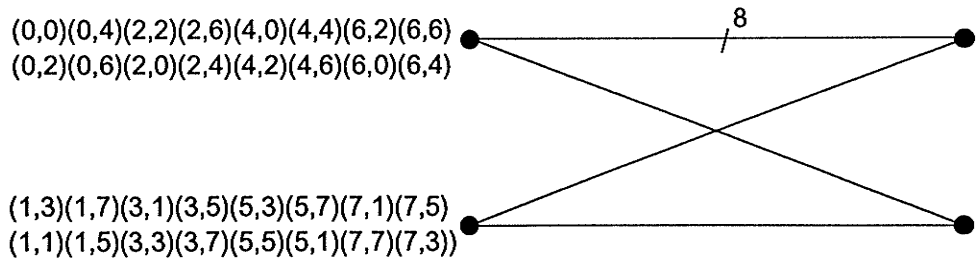

Figure 2.6 - Trellis for rate 4/6 MTCM scheme based on 8-PSK

The squared Euclidean distance between two parallel paths is the squared Euclidean distance between the two composite symbols assigned to these paths. In the example, the minimum squared Euclidean distance between parallel paths is represented by the squared Euclidean distance between the composite symbols (0,0) and (2,2) which equals $2d^2_{min}(0,2) = 2(2) = 4$. The minimum squared Euclidean distance for the error event that does not include parallel paths is the distance between the composite symbols (0,0) and (0,2) over the first branch of the error event and composite signals (0,0) and (1,3) over the second branch of the error event. The minimum squared Euclidean distance over this error event is

$$d^2_{min} = d^2[(0,0),(0,2)] + d^2[(0,0),(1,3)] = [0+2] + [4\sin^2\frac{\pi}{8} + 4\sin^2\frac{3\pi}{8}] = 6$$

Thus $d^2_{free} = 4$ for the error path length L=2. The asymptotic gain over uncoded QPSK is

$$\gamma = \frac{d^2_{free}}{d^2_{QPSK}} = \frac{4}{2} = 2 \quad \Rightarrow \quad 3\text{dB}$$

This represents a gain of 3-1.1=2.9 dB over the "standard" TCM scheme shown in Figure 2.2b. Furthermore, the two-state MTCM code has the same performance as the four-state TCM code for this signal set. Faster decoding is the advantage of keeping the number of states low and the two-state MTCM scheme is preferable to the four-state TCM scheme[4]. As a rule, an optimally designed MTCM code will always result in an increase in d^2_{free} compared to an optimum TCM code with the same number of states.

2.3.2 - Signal partitioning for MTCM

Signal partitioning for MTCM is different from that of TCM. Although the principle upon which the Ungerboeck partitioning is based still applies, the procedure is more complex since there are M^k composite symbols in the signal set. A useful partitioning technique has been developed by Divsalar and Simon [18] for the one-dimensional constellations M-AM and M-PSK[5]. Unfortunately, their technique is not directly adaptable to two-dimensional constellations such as M-QAM. For two-dimensional signal sets, the problem is identical to using a composite symbol set distributed in 2^k dimensional space. Furthermore, the composite symbol set does not necessarily fall on a lattice in 2^k space. Therefore, the partitioning techniques based on lattices and cossets developed by Calderbank and Sloane [9] cannot be used. More mundane techniques must therefore be applied. Two methods to partition two-dimensional signal sets were developed for this thesis. The first method is a brute force computer search that proved to be unwieldy for large signal sets. The second method also involves computer searches for larger signal sets although these searches are much more limited.

It is useful to visualise the signal set before conducting the partitioning. Since it is difficult to visualise a signal set in 2^k dimensional space, an alternative representation

---

[4] The decoding speed of the Viterbi algorithm usually decreases with increasing number of states.

[5] It should be noted however, that although signal partitioning is conducted differently from the Ungerboeck method, the three Ungerboeck rules that govern the mapping of subsets to trellises still apply.

must be chosen. Figure 2.7 is such a representation applied to 16-QAM with multiplicity k=2. It is basically a two-dimensional representation of the four-dimensional composite signal space. The 16-QAM signal set is duplicated and the duplicated copies are arranged into a 16-QAM configuration. Each duplicated signal set is referred to as a block. The individual symbols within a block are numbered from 0 to 15. Each block is also numbered from 0 to 15 following the same pattern. Since there are 16 blocks of 16 signals each, the full composite signal set contains 256 composite symbols. Each composite symbol is identified by two digits representing the block that contains it and its location within that block. For example, the composite symbol (3,5) is the composite symbol at position 5 in block 3.

The minimum squared Euclidean distance between two blocks is the same as the squared Euclidean distance between the two symbols in any block at the equivalent locations. For example, the squared Euclidean distance between block 0 and block 6 is the same as the squared Euclidean distance between symbol 0 and symbol 6 in any of the blocks. The squared Euclidean distance between two composite symbols is therefore equal to the sum of the squared Euclidean distance between their parent blocks and the squared Euclidean distance between the two signals calculated as if they were in the same block. For example, the squared Euclidean distance between composite symbol (2,3) and composite symbol (5,11) of Figure 2.7 is equal to

$$d^2 = d^2(2,5) + d^2(3,11)$$

The number of composite symbols in the composite signal set is twice the number of composite symbols required to design a MTCM scheme. The composite signal set must therefore be divided in half before the partitioning. In the optimum composite signal set, the minimum distance between the composite symbols should be as large as possible. Selecting every second composite symbol in each block will accomplish this. For example, if signal (0,0) of Figure 2.7 is chosen as part of the composite signal set, then rejecting all (odd,0) symbols in the block will maximize the minimum distance

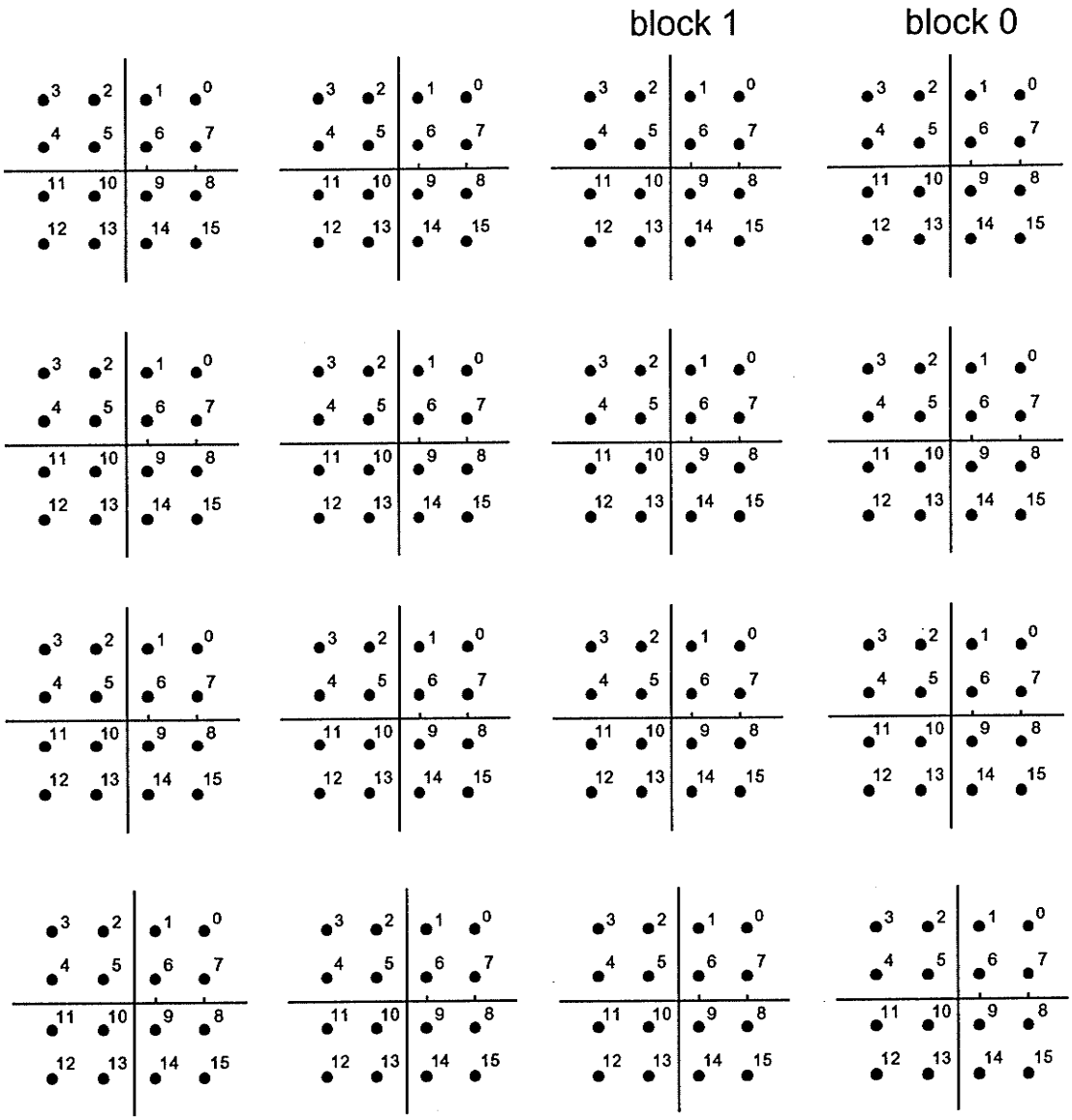

Figure 2.7 - Representation of 16-QAM signal set with k=2

between symbols in the block. The same is true for every block. In addition, if composite symbol (0,0) is selected as part of the composite signal set, then selecting composite symbol (1,1) will maximize the minimum distance between the composite symbols in the two adjacent blocks. Therefore, the composite signal set to be partitioned is formed by selecting all (even,even) and all (odd,odd) composite symbols in the original composite signal set. An equivalent composite signal set could also be formed by

selecting all (even,odd) and (odd,even) composite symbols in the original composite signal set.

Once the composite signal set has been selected, the set partitioning can be conducted. Two methods to conduct the partitioning are described below. Partitioning method 1 represents the brute force approach and its use is limited to smaller composite signal sets.. Partitioning method 2 is an alternate method that can be used to partition larger composite signal sets.

Partitioning method 1. The obvious method to partition the composite signal set is to by divide the composite symbols into two subsets at each lower level of partitioning. This partitioning is shown at Figure 2.8. Only one subset is shown for each successively lower partition level. Unlike the case for the partitioning of a multiplicity k=1 signal set, the squared Euclidean distance between composite symbols in a subset does not increase with each new level of partitioning. In fact, the first two levels of partitioning do not increase the squared Euclidean distance between composite signals in a partition. This is due to the fact that some composite symbols have 8 closest neighbours. Therefore, there is more than one equivalent way of partitioning subsets at level 1 and 2. For the case of 16-QAM, there are two equivalent ways of partitioning composite symbols into subsets at level 3. MTCM schemes based on these equivalent subsets will exhibit the same performance.

This first method of partitioning is cumbersome, especially for large numbers of composite symbols. To understand why, consider that the only information available to conduct the partitioning is the squared Euclidean distance between the composite symbols in a signal set. The maximum squared Euclidean distance possible between two subsets derived from this signal set may be also known. Assuming that this squared Euclidean inter-subset distance is known, the problem is to combine half the composite symbols into one subset so that the squared Euclidean intra-subset distance between the composite symbols in that subset is at least the squared Euclidean inter-subset distance. The

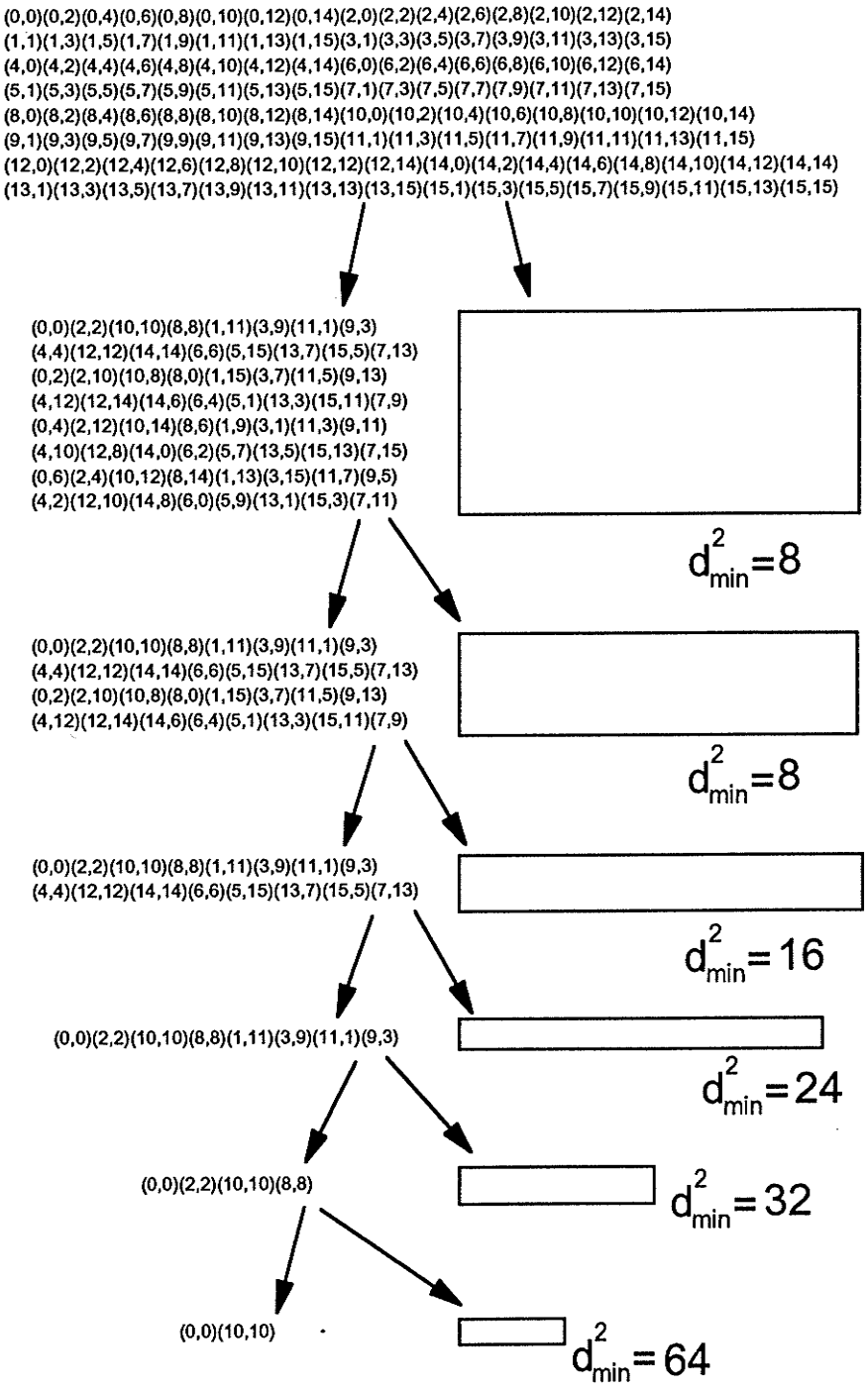

Figure 2.8 - Partitioning of 16-QAM composite signal set with k=2

second subset is then composed of the remaining composite symbols. Unfortunately, there is no guarantee that the squared Euclidean intra-subset distance between the composite symbols in the second subset will be higher than the squared Euclidean inter-subset distance. In most cases, the squared Euclidean intra-subset distance between composite symbols in the second subset will not be greater than the squared Euclidean inter-subset distance and the two subsets must be rejected. Furthermore, even if both subsets are acceptable, there is no guarantee that they will both partition into two sub-subsets where the squared Euclidean intra-distance between the composite symbols in each sub-subset is maximized. In fact, both subsets may not even partition into sub-subsets with the same minimum squared Euclidean intra-sub-subset distance.

Therefore, to ensure an optimum partitioning of the composite signal set, each acceptable subset at each level of partitioning must be analyzed individually. Since the number of subset combinations increases geometrically with the number of composite symbols, this method is unwieldy for large composite symbol sets. Experience has shown that partitioning a 16-signal set with a multiplicity of k=2 using this method is manageable. However, tackling a larger signal set would be very difficult.The next subsection describes an alternate partitioning method which is much simpler to implement. As a result, this second method of partitioning may be used for larger composite signal sets.

Partitioning method 2. In the second method of partitioning a MTCM two-dimensional composite signal set, the partitioning begins at the lower levels. Lower-level subsets are then combined into higher-level subsets. This method is referred to as the reverse partitioning method and is very.useful for designing trellis codes for the Rayleigh fading channel as shown in Chapter 3. The technique takes advantage of Ungerboeck partitioning of the basic signal set with multiplicity k=1. Figure 2.9 illustrates the Ungerboeck partitioning of a 16-QAM signal set. The subsets at the fourth level of partitioning represent symbol pairs with the greatest squared Euclidean distance

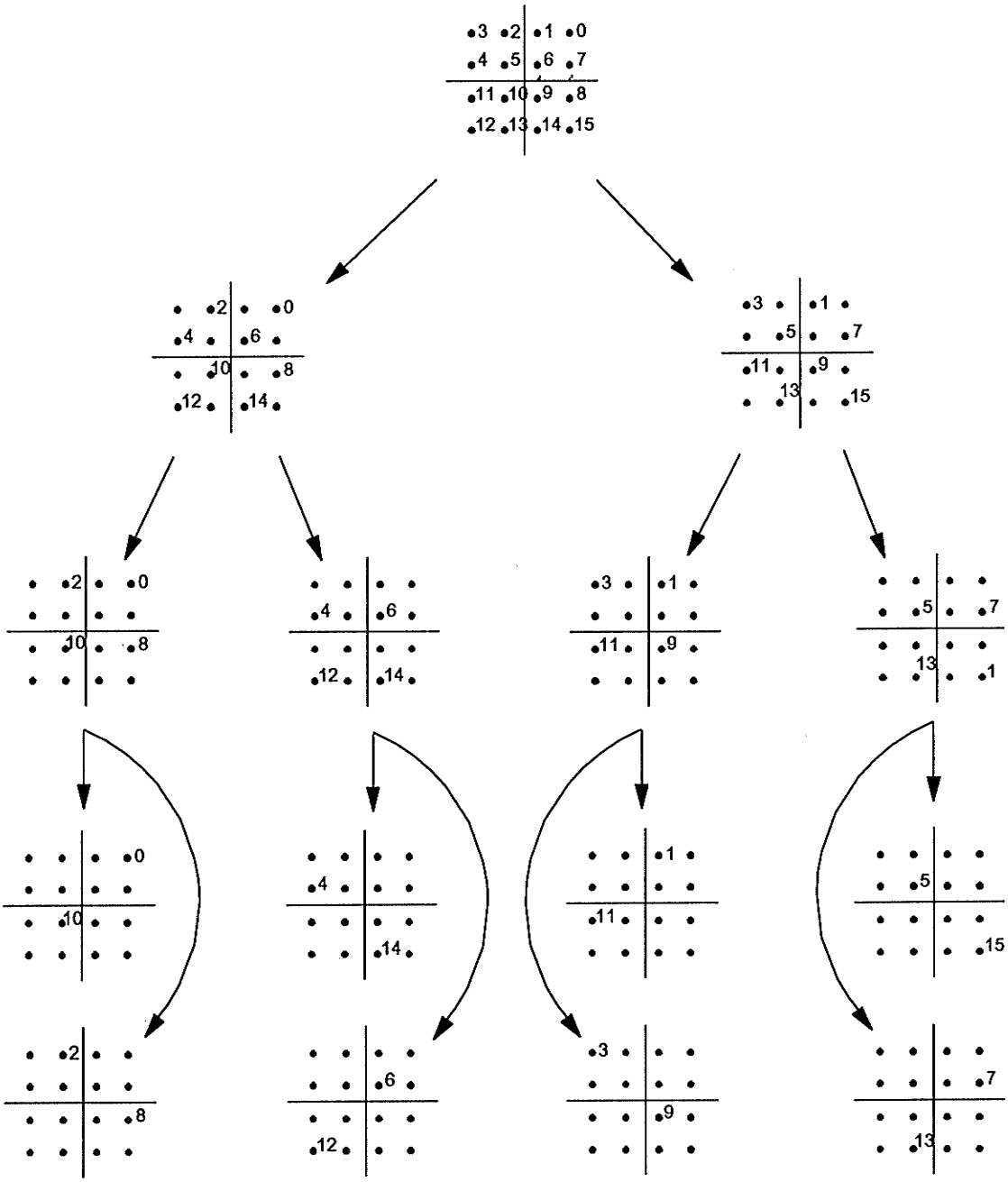

Figure 2.9 - Ungerboeck partitioning for 16-QAM

between them. These symbol pairs are called complement of each other. For example, symbol 8 is the complement of symbol 2.

The partitioning is conducted as follows. First, it must be determined which composite symbols should be paired together in a subset. Figure 2.9 shows how symbols in a block are paired together using Ungerboeck partitioning. One should therefore expect that a similar pattern exists for the composite symbol set and that composite symbols (0,0) and (10,10) should be complements. This is in fact the case as illustrated in Figure 2.8. Similarly, the composite symbols (2,2) and (8,8) are complements as are composite symbols (1,1) and (11,11). In this manner, it is easy to pair all composite symbols for which the constituent symbols repeat. This takes care of 16 composite symbols from our set of 128 composite symbols.

Pairing the remaining 112 composite symbols is equally simple. Consider the composite symbol (2,14). The complement of (2,14) is the composite symbol whose first symbol is the complement of 2 and whose second symbol is the complement of 14 or (8,4). The squared Euclidean distance between the two composite symbols is obviously the same as the squared Euclidean distance between (0,0) and (10,10). All remaining 110 composite symbols in the composite signal set may be paired in this fashion.

Once all composite symbol complements have been identified, they must be combined into subsets at the next higher level of partitioning. For larger composite symbol sets, this is best accomplished through computer searches. In the current example, this process leads to 64 subsets of four composite symbols each including the subset {(0,0)(2,2)(8,8)(10,10)}. At this level of partitioning, the subset made up of composite symbols (0,4) and (10,14) will be combined with the subset made up of composite symbols (2,12) and (8,6) or the subset made up of composite symbols (2,6) and (8,12). Both combinations are equivalent. Once all subsets at a partitioning level have been identified, the process is repeated at each successively higher partitioning level until the original composite symbol set is obtained at level 0.

This second method of partitioning is much quicker than the first partitioning method. Since the lower-level subsets are known, there is no ambiguity in selecting the higher-level subsets. There may be more than one way of combining lower-level subsets into higher-level subsets but the resulting subsets are truly equivalent and only one solution needs to be retained. Because of its simplicity, this partitioning method will handle large composite signal sets. Although 64-QAM with a multiplicity k=2 is the largest composite signal set partitioned for this thesis, partitioning 128-SQ or 256-QAM should be straightforward.

2.3.3 - Example: 4-states, rate 6/8 MTCM scheme based on 16-QAM

The following example of a multiplicity k=2, 4-state MTCM scheme based on a 16-QAM signal set illustrates MTCM for a two-dimensional signal set. The trellis for this scheme is fully connected, meaning that each state is connected to all the other states by a branch. Since 64 composite symbols are required to represent all possible input bit combinations, there are 16 parallel paths for each branch. The signal partitioning for 16-QAM was conducted in the last section and is shown at Figure 2.8. The optimum mapping is conducted using the three Ungerboeck rules and is illustrated at Figure 2.10. In this trellis, each (An), $1 \leq n \leq 8$, represents the eight composite symbols assigned to the same path. The various composite symbols represented by (An) are shown at the right of the trellis.

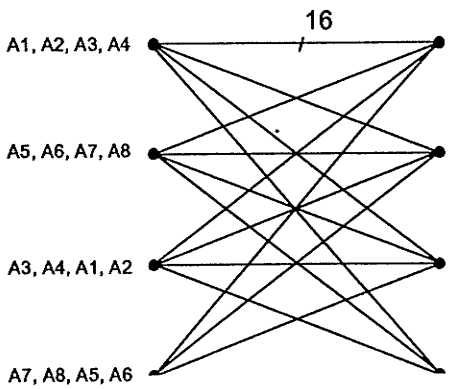

A1-{0,0}{2,2}{10,10}{8,8}{1,11}{3,9}{11,1}{9,3}
{4,4}{12,12}{14,14}{6,6}{5,15}{13,7}{15,5}{7,13}
A2-{0,2}{2,10}{10,8}{8,0}{1,15}{3,7}{11,5}{9,13}
{4,12}{12,14}{14,6}{6,4}{5,1}{13,3}{15,11}{7,9}
A3-{0,4}{2,12}{10,14}{8,6}{1,9}{3,1}{11,3}{9,11}
{4,10}{12,8}{14,0}{6,2}{5,7}{13,5}{13,15}{7,13}
A4-{0,6}{2,4}{10,12}{8,14}{1,13}{3,15}{11,7}{9,5}
{4,2}{12,10}{14,8}{6,0}{5,9}{13,1}{15,3}{7,11}
A5-{0,8}{2,0}{10,2}{8,10}{1,5}{3,13}{11,15}{9,7}
{4,6}{12,4}{14,12}{6,14}{5,11}{13,9}{15,1}{7,3}
A6-{0,10}{2,8}{10,0}{8,2}{1,1}{3,3}{11,11}{9,9}
{4,14}{12,6}{14,4}{6,12}{5,5}{13,13}{15,15}{7,7}
A7-{0,12}{2,14}{10,6}{8,4}{1,7}{3,5}{11,13}{9,15}
{4,8}{12,0}{14,2}{6,10}{5,3}{13,11}{15-9}{7,1}
A8-{0,14}{2,6}{10,4}{8,12}{1,3}{3,11}{11,9}{9,1}
{4,0}{12,2}{14,10}{6,8}{5,13}{13,15}{15,7}{7,5}

Figure 2.10 - Rate 6/8 MTCM scheme based on 16-QAM

The free distance for the code can be determined by examining the trellis. The composite symbols assigned to parallel paths differ in both components and the error event length over the parallel path is therefore L=2. The minimum squared Euclidean distance over the parallel paths is represented by composite symbols (10,10) and (5,15) and is

$$d^2_{min} = d^2(10,5) + d^2(10,15) = 4 + 20 = 24$$

The error event length, disregarding parallel paths, is L=3 and is represented by composite symbols (10,10) and (10,8) for the first transition and composite symbols (10,10) and (6,14) for the second transition. The minimum squared Euclidean distance over this error event is:

$$d^2_{min} = d^2(10,10) + d^2(10,8) + d^2(10,6) + d^2 10,14) = 0 + 16 + 8 + 8 = 32$$

The free distance of the code is therefore $d^2_{free} = 24$ and the asymptotic gain compared to uncoded QPSK is

$$\gamma = \frac{d^2_{free}/E_{16QAM}}{d^2_{QPSK}/E_{QPSK}} = \frac{24/10}{2/1} = 1.2 \quad \Rightarrow \quad 0.79\,dB$$

Although this result represents only a small improvement in P[error] over uncoded QPSK, the information throughput of this scheme is 3 bits per symbol versus 2 bits per symbol for uncoded QPSK or 1.5 times higher than uncoded QPSK.

2.4 - Summary

The performance of a TCM or a MTCM scheme depends on how the symbols are mapped to the various paths in the trellis. For an optimum scheme, the signal set must be partitioned in such a way that the minimum squared Euclidean distance between symbols in each subset is maximized, regardless of the level of partitioning. In addition, these subsets must be mapped into the various branches in the trellis in such a way as to

maximize the d_{free}^2 of the trellis. A failure to satisfy either one of these two conditions leads to a less than optimum code.

Two partitioning methods were developed to partition a two-dimensional signal set for MTCM. Of these two methods, the reverse partitioning method is clearly superior and will be used to design MTCM schemes for the Rayleigh fading channel in Chapter 3.

Chapter 3 - TCM and MTCM schemes for the Rayleigh fading channel

3.1 - General

Although maximizing the free Euclidean distance d_{free} of a TCM scheme is the main design criterion for the AWGN channel, Divsalar and Simon [19,20] have shown that the asymptotic performance of TCM for the Rayleigh fading channel is governed by other factors. Section 3.2 examines these factors and discusses their implications in the design of TCM and MTCM schemes for the Rayleigh fading channel. An extension of the reverse partitioning method previously discussed in section 2.3.3 is developed for the Rayleigh fading channel in section 3.3. In section 3.4, the reverse partitioning method is used to design various TCM and MTCM schemes based on two-dimensional signal sets for the Rayleigh fading channel. Section 3.5 analyses the effect of increasing the multiplicity of an MTCM scheme designed for the Rayleigh fading channel.

3.2 - Criteria for designing TCM and MTCM schemes for the Rayleigh fading channel

Divsalar and Simon [19] have derived an asymptotic upper bound on the pairwise error probability $P(x \rightarrow \hat{x})$ for TCM and MTCM schemes based on M-PSK for the Rayleigh fading channel. The pairwise error probability represents the probability of choosing the coded sequence $\hat{\mathbf{x}} = (\hat{x}_1, \hat{x}_2, ..., \hat{x}_N)$ when $\mathbf{x} = (x_1, x_2, ..., x_N)$ is transmitted. This upper bound is given by:

$$P(x \rightarrow \hat{x}) \leq \left(\prod_n [1 + \frac{E_s}{4N_o} |x_n - \hat{x}_n|^2] \right)^{-1} \qquad (3.1)$$

At sufficiently high SNR, equation (3.1) simplifies to the asymptotic case

$$P(x \rightarrow \hat{x}) \leq \left(\prod_n \frac{E_s}{4N_o} |x_n - \hat{x}_n|^2 \right)^{-1} ;;;; \qquad (3.2)$$

Cavers and Ho [12] have shown that the pairwise error probability for other signal sets has the form of equation 3.2 multiplied by a correction factor. The following discussion therefore applies to all signal sets. $P(x \rightarrow \hat{x})$ is inversely proportional to the product of the squared Euclidean distance along the error path. Therefore, the primary design criterion for high signal-to-noise ratios (SNR) is the maximization of the length of the shortest error event path L. The maximization of the product of the branch distances along that path is the second design criterion. A TCM or MTCM scheme that meets both of these criteria will perform optimally over the Rayleigh fading channel even through d_{free} does not achieve its optimum value over the AWGN channel.

The primary design criterion for the Raleigh fading channel introduces an important limitation in the design of TCM schemes. Since the performance of the code is inversely proportional to the length of the minimum error event path, trellises which contain a parallel path (L=1), will perform poorly over this type of channel. This in turn implies that trellises based on large M must have many states to avoid these parallel paths. For example, the minimum number of states for trellises based on 16-QAM and 64-QAM signal sets must be 8 and 32 respectively in order to avoid parallel paths. On the other hand, it is important to limit the number of states in trellises for mobile radio communications because the complexity of the decoder increases with the number of states. An increase in decoder complexity results in additional cost and longer decoding delays, both of which are undesirable. A search through recent scientific literature indicates that most authors consider 8-state trellises [21,22] as practical for mobile radio communications while 16-state trellises have not been considered seriously.

It is not possible to reconcile these conflicting criteria solely through using standard TCM schemes for large signal sets. However, the minimum error event length in a trellis can be increased by using MTCM even though parallel paths are present. Most of the schemes developed in this thesis have 8 states due to the practical considerations discussed above. There is some discussion on 16-state schemes but optimum trellises for

these schemes are not provided because the search for 16-state optimum trellises is difficult and requires extensive computer searches.

The following example extracted from [20] illustrates the design criteria for the design of MTCM schemes for the Rayleigh fading channel. Consider the trellis diagram of Figure 3.1 for the k=2, rate 4/6 MTCM scheme for 8-PSK.

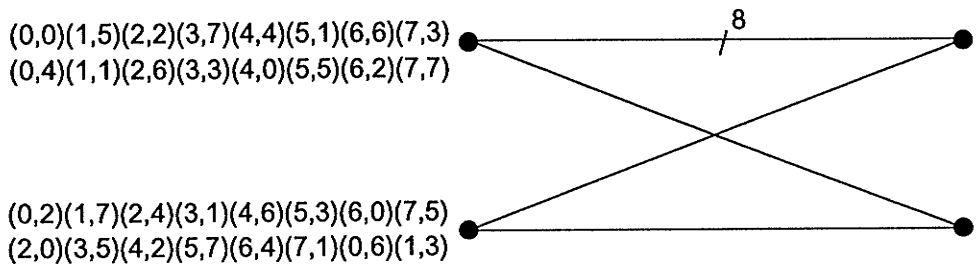

Figure 3.1 - Rate 4/6 MTCM based on 8-PSK for the Rayleigh fading channel

The signal set can be found in Figure 2.2a. Observe that in order for the minimum error event length to be larger than one, the composite signals assigned to parallel paths must differ in both symbol positions. This holds true for the example and the minimum error event path for that MTCM scheme is L=2. This fulfils the principal design criterion. The second design criterion requires that the product of the squared distance over the minimum error event path be maximized. In the example, if the all-zero path is arbitrarily taken as the correct one, the minimum product over the error event path of length L=2 for the parallel paths is represented by composite symbols (0,0) and (1,5) and is equal to

$$d^2 = d^2[(0,0),(1,5)]$$

$$= d^2(0,1) \bullet d^2(0,5) = 4\sin^2\frac{\pi}{8} \bullet 4\sin^2\frac{5\pi}{8} = (.5858)(3.4142) = 2$$

For the two-branch error event path of L=2, this error event is represented by composite symbols (0,0) and (0,4) over the first branch and composite symbols (0,0) and (0,2) over the second branch. The minimum product over this path is equal to[2]

$$d^2 = d^2[(0,0),(0,2)] \bullet d^2[(0,0),(1,3)]$$

$$= d^2(0,0) \bullet d^2(0,4) \bullet d^2(0,0) \bullet d^2(0,2) = 4 \bullet 2 = 8$$

Since the product for the parallel branches is the smallest, the performance of the scheme will be determined by that product. In this example, the minimum squared distance over the minimum error event path has already been maximized and this trellis is optimum in the sense that no other signal assignment can yield a better error performance.

It is relatively simple to design a MTCM scheme that only meets the primary design criterion for the Rayleigh fading channel. However, the error performance of such an arbitrary scheme would likely be poor. Therefore, it would be preferable to design MTCM schemes that meet both design criteria. Partitioning the composite signal set in such a way as to meet the second design criterion is complex but possible. This problem is resolved in the next section.

3.3 - Signal partitioning for the Rayleigh fading channel

Divsalar and Simon have developed a method to partition M-PSK signal sets for the Rayleigh fading channel. The technique can be used for various values of k and takes advantage of the high degree of symmetry in M-PSK constellations. However, the distance between symbols in an M-PSK signal set decreases rapidly with M. Accordingly, increasing the size of the signal set results in a rapidly diminishing return in performance. For large signal sets, two-dimensional constellations like M-QAM are preferable.

---

[2] Note that the pairwize error probability expression given at Equation 3.1 guaranties that each term in the product is at least 1. Therefore, the distance between two identical symbols is considered to be 1 in all distance calculations involving a scheme designed for the Rayleigh fading channel.

Unfortunately, partitioning signal sets for these constellations is difficult because of the lack of symmetry within these signal sets.

This thesis results in the partitioning of various constellations including 8-, 16- and 32-QAM as well as 8- and 32-SQ for the Rayleigh fading channel[3]. This partitioning is conducted using the reverse partitioning method described in section 2.3.3 combined with computer searches for the larger signal sets. A multiplicity of k=2 is assumed throughout except when specifically stated otherwise.

The reverse partitioning method relies on the fact that the lower-level partitions are known. These partitions are easily derived for the AWGN channel as discussed in Chapter 2. However, the lower-level partitions for the Rayleigh fading channel are not immediately obvious because the partitioning criteria differ from the one for the AWGN channel. Therefore, it may appear that the partitioning of M-QAM signal sets for the Rayleigh fading channel is complex. In fact, this is not true and it can be shown that the lower-level partitions for the Rayleigh fading channel are identical to the lower-level partitions for the AWGN channel for many signal constellations. As proof, the following lemma is used:

Lemma 3.1. The lower level of partitioning for the Rayleigh fading channel is the same as the lower level of partitioning for the AWGN channel for M-SQ signal sets and for M-QAM signal sets where $M=2^s$, s even.

Proof. To prove that this lemma is valid, it must satisfy both performance criteria for a MTCM code designed for the Rayleigh fading channel. Partitioning a M-QAM or a M-SQ constellation using the partitioning method described in section 2.3.3 will always satisfy the

[3] SQ refers to skewed quadrature. A SQ signal set is a signal set that includes every second symbol of a squared M-QAM signal set. For example, 32-SQ contains every second symbol of 64-QAM.

primary criterion since the two composite symbols at the lower level of partitioning differ in both symbol positions.

The second criterion can be verified as follows: Consider two numbers a and b such that their sum is a+b=c. Then a=c-b. Let the product ab=d or (c-b)b=d. This product is maximized when the derivative of d with respect to b is zero, that is: 0=c-2b. This implies that 2b=c or that a=b. For the Ungerboeck partitioning of a composite M-QAM or a M-SQ signal set, the squared Euclidean distance between constituent symbols of the two composite signals at the lower level of partitioning are identical. Therefore, the product of the squared Euclidean distance between the two composite signals is maximized. This effectively satisfies the second criterion.

By taking advantage of the above lemma, the reverse partitioning of the composite signal set for the Rayleigh fading channel is considerably facilitated because the lower-level partitions can be designed as if they were intended for the AWGN channel. They can then be combined into higher-level partitions according to the design criteria for the Rayleigh fading channel.

The reverse partitioning method for the Rayleigh fading channel applies to all squared signal sets, that is, signal sets where the symbols in the set can be circumscribed by a square. For example, the rule applies to 16- and 64-QAM as well as 8- and 32-SQ signal sets. The rule also applies to other (but not all) signal sets such as 8- and 32-QAM which are not circumscribed by a square.

3.4 - Designing MTCM schemes for the Rayleigh fading channel

3.4.1 - General

This section deals with the design of MTCM schemes based on two-dimensional signal sets with a multiplicity of k=2 for the Rayleigh fading channel. The reverse partitioning method is applied to 8- and 32-SQ as well as 8-, 16- and 64-QAM signal sets. The results of the partitioning are then applied in the design of MTCM schemes optimally suited to the Rayleigh fading channel. These schemes are discussed in sub-sections 3.4.2 through 3.4.6.

All the schemes discussed in this thesis have 8 or fewer states. It would have been useful to design MTCM schemes for larger trellises. However, designing optimum trellises becomes increasingly difficult as the number of states is increased. This is because there exist no easy method to design optimum trellises other than exhaustive computer searches. The number of possible mappings increases rapidly with the number of states making these searches lengthy.

The error performance of the MTCM schemes designed in this section were simulated on a GATEWAY 2000 4DX2-66 IBM compatible computer. The software was written in C++ and compiled with the Borland C++ compiler. The simulations used a multipurpose Viterbi decoder capable of handling schemes based on any of the signal sets and multiplicity considered in this thesis. The Viterbi decoder software was not optimized for any particular scheme. The various data points are based on simulations producing at least 1,000 symbol errors. Sub-section 3.4.7 compares the relative processing times for some of the schemes designed in this section.

3.4.2 - 8-SQ, multiplicity k=2

Consider a 8-SQ, k=2 signal set as shown in figure 3.2. There are (8)(8)=64 composite symbols of which only 32 are required to represent all combinations of information bit pairs. No trellis based on this signal set may have more than 8 parallel paths or the primary design criterion for the Rayleigh fading channel would not be met. Therefore, it is sufficient to partition the signal set in such a way that the highest-level partitions do not contain more than 8 composite symbols. Accordingly, the highest-level partition is divided into 4 partitions of 8 composite symbols each. The partitioning for both the AWGN and the Rayleigh fading channel is shown in Figure 3.3.

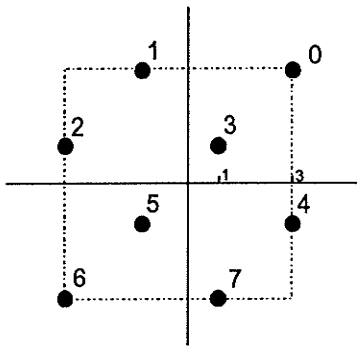

Figure 3.2 - 8-SQ signal set

The composite symbols in the lower-level partitions are selected according to the complement rule discussed in section 2.3.3. These 32 individual composite symbols are shown in column 1 of Figure 3.3. Column 2 of Figure 3.3 shows the pairs of composite symbols at the lowest level of partitioning. Lemma 3.1 ensures that the product of the squared Euclidean distance between these pairs of composite symbols is maximized. In the third column, the partitions in column 2 are combined into a higher-level partition according to the criterion for the AWGN channel. Since the constituent symbols of the composite symbol pairs at this level of partitioning differ in both positions, both design criteria for the Rayleigh fading channel are also met. Therefore, the partitioning of column 3 is optimal for both types of channel.

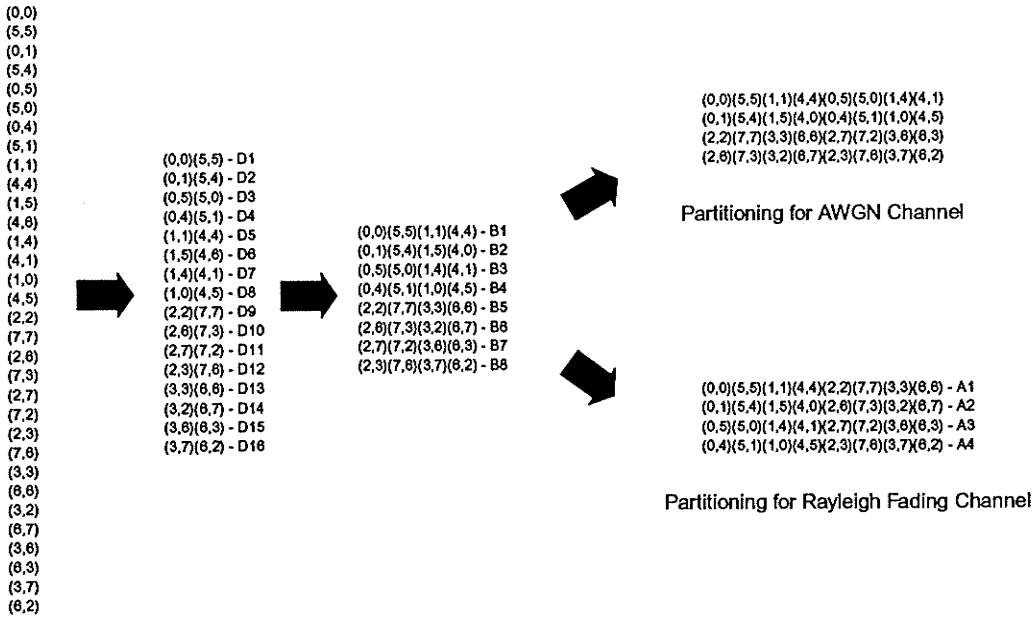

Figure 3.3 - Partitioning of 8-SQ with k=2

The fourth column shows the optimum partitioning at the last level of partitioning that is of interest for the AWGN and the Rayleigh fading channel. The two sets of subsets differ. Indeed, it is apparent that the optimum subsets for the AWGN channel contradict the primary design criterion for the Rayleigh fading channel. The optimum subsets for the Rayleigh fading channel therefore differ as shown. As a result, trellises based on the Rayleigh fading channel are not optimum for the AWGN channel and vice versa.

Figure 3.4 illustrates optimum trellises for 2-, 4- and 8-state MTCM for the 8-SQ signal set. The symbol error performance of these schemes were simulated and the results are shown in Figure 3.5. The performance of these MTCM schemes increases with the number of states. Also shown is the symbol error performance of an optimum 8-state, half-connected TCM scheme, i.e., with a multiplicity k=1. The minimum error event length for that scheme is L=3. The symbol error performance of that TCM scheme is superior to that of the equivalent MTCM scheme. Therefore, there is no advantage in

using an 8-state MTCM scheme for a signal set with M=8 since the equivalent TCM scheme is superior.

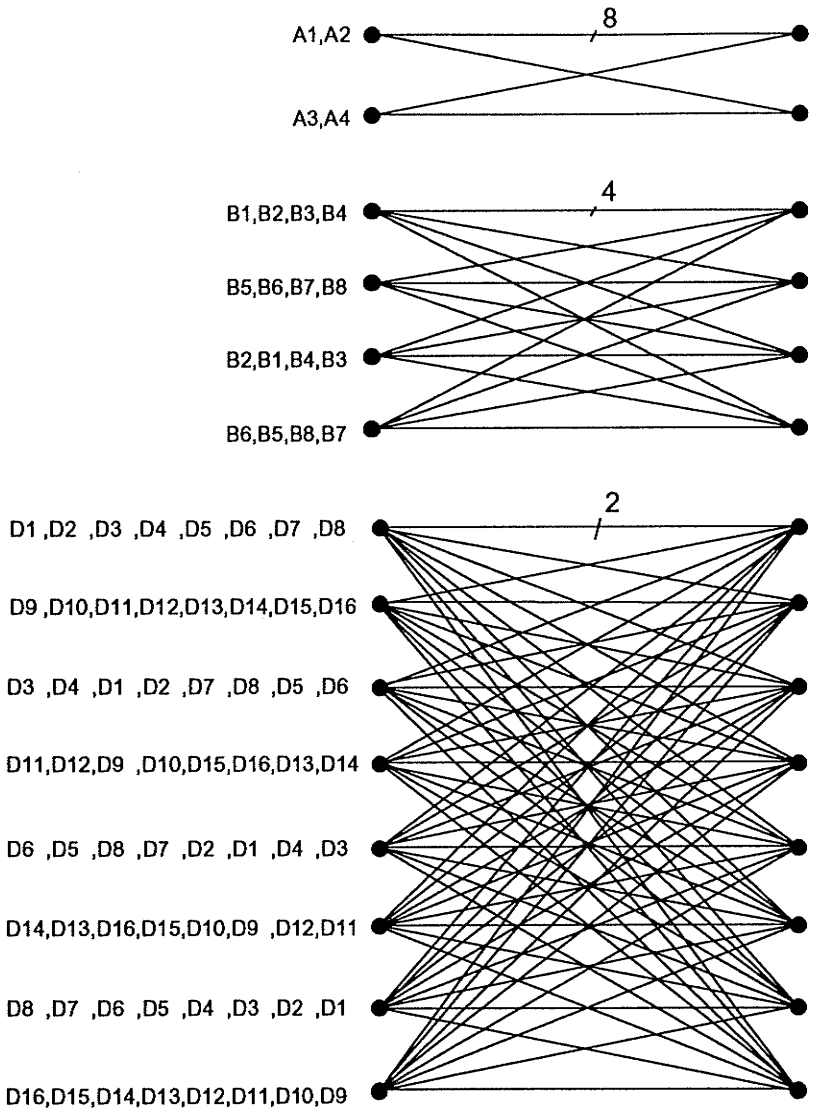

Figure 3.4 - Trellises for MTCM schemes based on 8-SQ

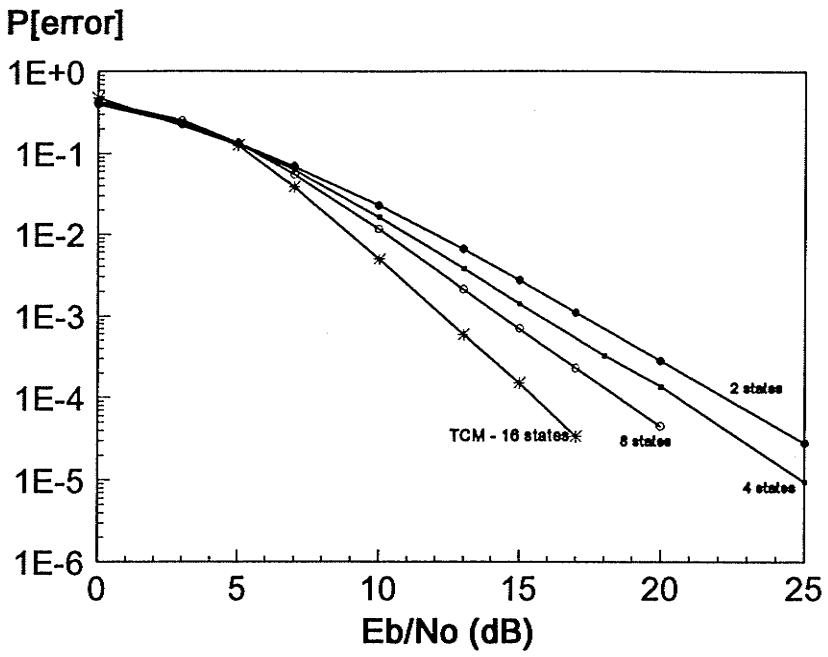

Figure 3.5 - P[error] in a Rayleigh fading channel for TCM and MTCM schemes based on 8-SQ

3.4.3 - 8-QAM, multiplicity k=2

The partitioning rule described in section 3.3 may be applied to 8-QAM even though that signal set is not circumscribed by a square. 8-QAM is a special case and works because there are only 8 symbols in the signal set. The same is not true for 32-QAM. Figure 3.6 shows the partitioning of the composite signal set for the AWGN channel. This partitioning does not contradict either design criterion for MTCM schemes for the Rayleigh fading channel. Therefore, the optimum partitioning is identical for both channels. The trellis for the optimum 2-state MTCM scheme based on 8-QAM is identical to the 2-state trellis of figure 2.4.

Figure 3.7 plots the symbol error performance of optimum 2-state MTCM schemes based on 8-QAM, 8-SQ and 8-PSK. As shown, the symbol error performance of the optimum MTCM scheme based on 8-PSK is inferior compared to the symbol error

performance of the other two schemes. The difference between the performance of the schemes based on 8-SQ and 8-QAM is less than 0.2 dB at a symbol error rate of 10^{-3}.

For larger M, the symbol error performance of schemes based on M-PSK is also expected to be inferior to schemes based on M-QAM or M-SQ signal sets since the distance between the closest symbols in M-PSK diminishes faster for increasingly larger M than in the case for the other two signal sets. For this reason, this thesis does not further compare the performance of MTCM schemes based on M-PSK against the performance of MTCM schemes based on two-dimensional signal sets.

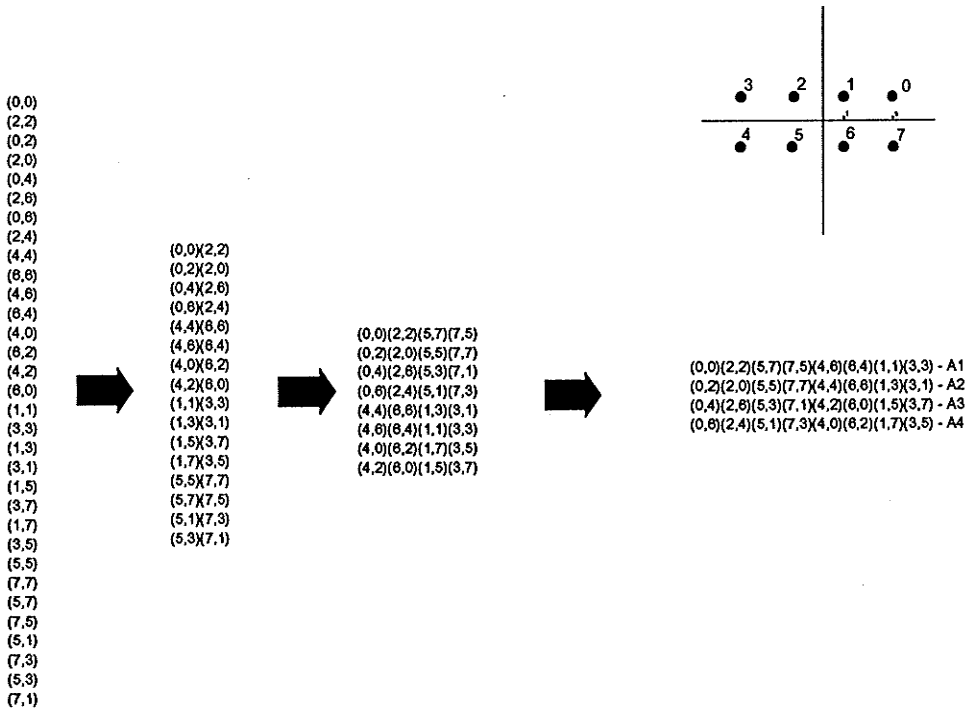

Figure 3.6 - Partitioning of 8-QAM with k=2

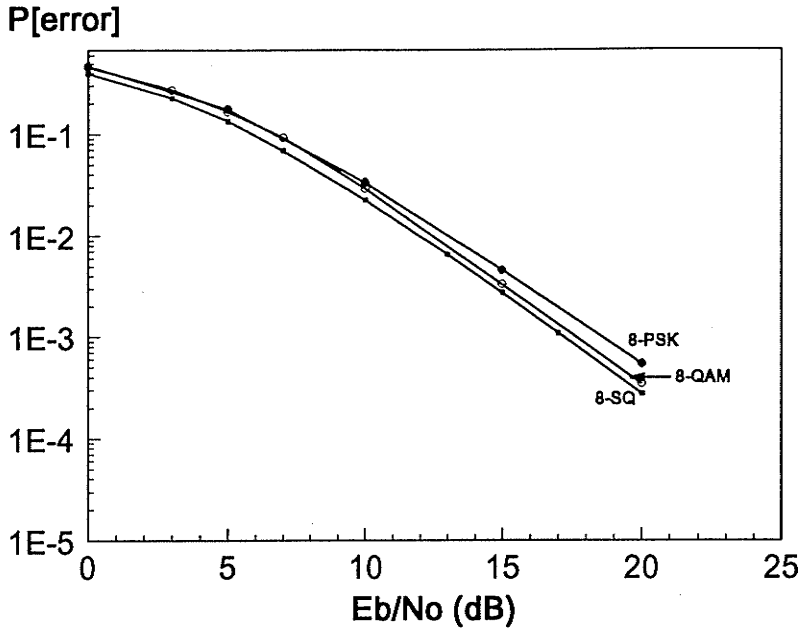

Figure 3.7 - P[error] in a Rayleigh fading channel for 2-state MTCM schemes based on 8-QAM, 8-SQ and 8-PSK

3.4.4 - 16-QAM, multiplicity k=2

The use of 16-QAM increases the information throughput by one bit per signalling interval compared to schemes based on signal sets with 8 symbols. In the case of a M=16 signal set such as 16-QAM, there are (16)(16)=256 composite symbols of which only half, or 128, are required for the scheme. Since there cannot be more than 16 parallel paths in order to meet the primary design criterion for the Rayleigh fading channel, schemes based on 16-QAM must have trellises with at least 4 states. It is therefore sufficient to partition the composite signal set into 8 partitions of 16 composite signals each at the highest level of partitioning. The optimum partitioning for the Rayleigh fading channel is shown in Figure 3.8 at the appropriate levels for the 4- and 8-state schemes. The 16-QAM composite signal set can be found in figure 2.7.

(0,0)(2,2)(10,10)(8,8)(1,11)(3,9)(11,1)(9,3) - B1
(4,4)(12,12)(14,14)(6,6)(5,15)(13,7)(15,5)(7,13) - B2
(0,2)(2,10)(10,8)(8,0)(1,15)(3,7)(11,5)(9,13) - B3
(4,12)(12,14)(14,6)(6,4)(5,1)(13,3)(15,11)(7,9) - B4
(0,4)(2,12)(10,14)(8,6)(1,9)(3,1)(11,3)(9,11) - B5
(4,10)(12,8)(14,0)(6,2)(5,7)(13,5)(15,13)(7,15) - B6
(0,6)(2,4)(10,12)(8,14)(1,13)(3,15)(11,7)(9,5) - B7
(4,2)(12,10)(14,8)(6,0)(5,9)(13,1)(15,3)(7,11) - B8
(0,8)(2,0)(10,2)(8,10)(1,5)(3,13)(11,15)(9,7) - B9
(4,6)(12,4)(14,12)(6,14)(5,11)(13,9)(15,1)(7,3) - B10
(0,10)(2,8)(10,0)(8,2)(1,1)(3,3)(11,11)(9,9) - B11
(4,14)(12,6)(14,4)(6,12)(5,5)(13,13)(15,15)(7,7) - B12
(0,12)(2,14)(10,6)(8,4)(1,7)(3,5)(11,13)(9,15) - B13
(4,8)(12,0)(14,2)(6,10)(5,3)(13,11)(15,9)(7,1) - B14
(0,14)(2,6)(10,4)(8,12)(1,3)(3,11)(11,9)(9,1) - B15
(4,0)(12,2)(14,10)(6,8)(5,13)(13,15)(15,7)(7,5) - B16

(0,0)(2,2)(10,10)(8,8)(1,11)(3,9)(11,1)(9,3)(4,4)(12,12)(14,14)(6,6)(5,15)(13,7)(15,5)(7,13) - A1
(0,2)(2,10)(10,8)(8,0)(1,15)(3,7)(11,5)(9,13)(4,12)(12,14)(14,6)(6,4)(5,1)(13,3)(15,11)(7,9) - A2
(0,4)(2,12)(10,14)(8,6)(1,9)(3,1)(11,3)(9,11)(4,10)(12,8)(14,0)(6,2)(5,7)(13,5)(15,13)(7,15) - A3
(0,6)(2,4)(10,12)(8,14)(1,13)(3,15)(11,7)(9,5)(4,2)(12,10)(14,8)(6,0)(5,9)(13,1)(15,3)(7,11) - A4
(0,8)(2,0)(10,2)(8,10)(1,5)(3,13)(11,15)(9,7)(4,6)(12,4)(14,12)(6,14)(5,11)(13,9)(15,1)(7,3) - A5
(0,10)(2,8)(10,0)(8,2)(1,1)(3,3)(11,11)(9,9)(4,14)(12,6)(14,4)(6,12)(5,5)(13,13)(15,15)(7,7) - A6
(0,12)(2,14)(10,6)(8,4)(1,7)(3,5)(11,13)(9,15)(4,8)(12,0)(14,2)(6,10)(5,3)(13,11)(15,9)(7,1) - A7
(0,14)(2,6)(10,4)(8,12)(1,3)(3,11)(11,9)(9,1)(4,0)(12,2)(14,10)(6,8)(5,13)(13,15)(15,7)(7,5) - A8

Figure 3.8 - Partitioning of 16-QAM with k=2

Optimum 4- and 8-state MTCM schemes based on 16-QAM are shown in Figure 3.9 using the partitions in Figure 3.8. The simulation results for these two schemes are shown in Figure 3.10. At a P[error] of 2×10^{-3} the 8-state scheme is approximately 1 dB better than the 4-state scheme. This value is verified using equation 3.1. The asymptotic symbol error performance of the 4-state scheme is determined by the product of the squared Euclidean distance between composite symbols assigned to parallel paths which is

$$P[\text{error}] \propto \frac{16}{(E/N_0)^2} \bullet \frac{1}{8 \bullet 8} = \frac{1}{4(E/N_0)^2}$$

By comparison, the asymptotic symbol error performance of the optimum 8-state MTCM scheme shown is also restricted by parallel paths and is

$$P[\text{error}] \propto \frac{16}{(E/N_0)^2} \bullet \frac{1}{4 \bullet 20} = \frac{1}{5(E/N_0)^2}$$

which represents an improvement of approximately 0.97 dB over the 4-state MTCM scheme. This value confirms the results of the simulations. Furthermore, it confirms that equation 3.2 is relatively accurate when comparing the performance of two schemes based on the same signal set. However, equation 3.2 is not accurate when comparing the performance of two schemes based on different signal sets. This is not surprising since the correction factors applied to equation 3.2 are different for each signal set as previously stated in section 3.2.

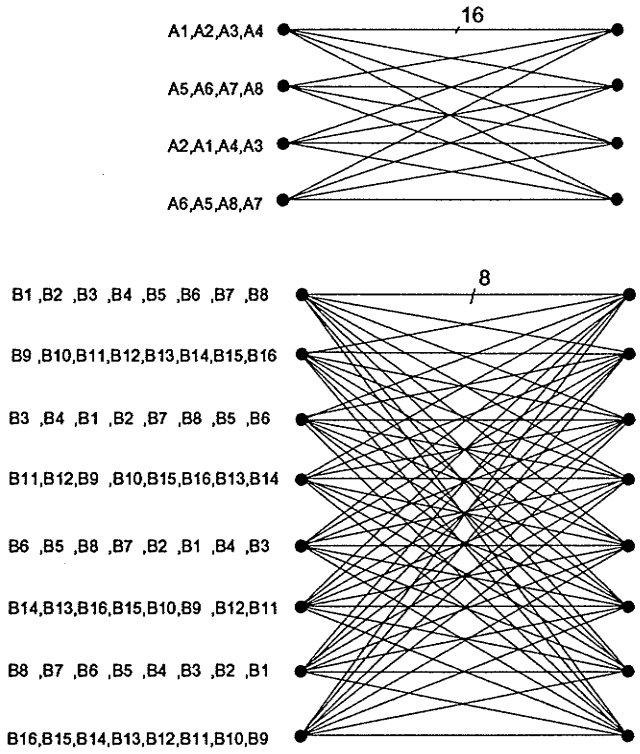

Figure 3.9 - Trellises for MTCM schemes based on 16-QAM

Although an optimum 16-state MTCM scheme was not designed, the symbol error performance of that scheme may be estimated by comparison to the 4- and 8-state

schemes using equation 3.1. Assuming that the parallel paths govern the symbol error performance, we get

$$P[\text{error}] \propto \frac{16}{(E/N_0)^2} \bullet \frac{1}{16 \bullet 16} = \frac{1}{16(E/N_0)^2}$$

which represents an improvement in error performance of 5.5 dB over the 8-state scheme. This is a significant improvement.

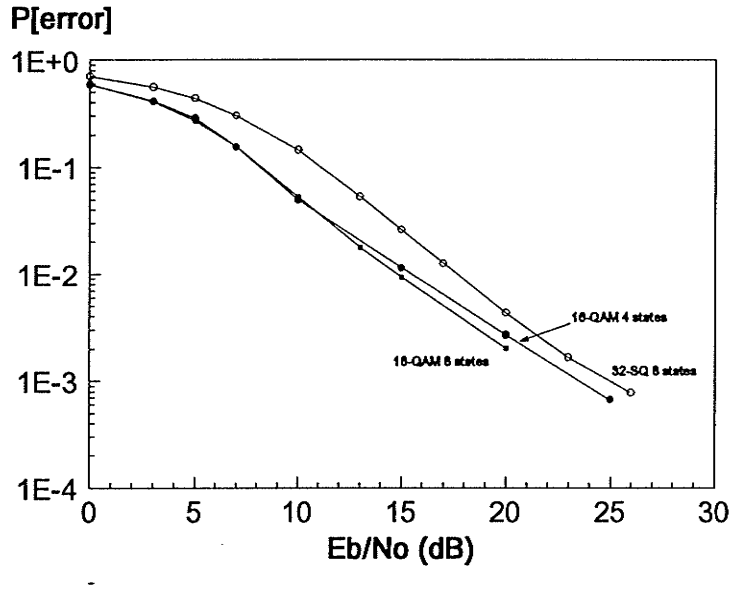

Figure 3.10 - P[error] in a Rayleigh fading channel for MTCM schemes based on 16-QAM and 32-SQ

A conventional TCM scheme based on 16-QAM requires 8 states to avoid parallel paths. However, the error event length for such a trellis is only L=2. In order to increase the error event length to L=3 and make a conventional code competitive with MTCM schemes, a trellis with 64 states would be required. Such a trellis is beyond the scope of this thesis. The performance of the 8-state conventional TCM scheme is estimated through equation 3.1

$$P[\text{error}] \propto \frac{16}{(E/N_0)^2} \bullet \frac{1}{16 \bullet 4} = \frac{1}{4(E/N_0)^2}$$

The error performance of this scheme is identical to the error performance of the 4-state MTCM scheme[4]. Because of its lower number of states, the four-state MTCM scheme is preferable to the 8-state conventional TCM scheme.

3.4.5 - 32-SQ, multiplicity k=2

32-SQ is illustrative of signal sets with 32 symbols. There are 1,024 composite symbols of which 512 are required for MTCM schemes. This implies that there are 256 composite symbols for every node of the trellis. Since there cannot be more than 32 parallel paths in order to meet the primary design criterion for the Rayleigh fading channel, trellises with less than 8 states need not be considered. The highest level of partitioning will therefore contain 16 partitions of 32 composite symbols each. These 16 partitions are shown in figure 3.11.

The optimum 8-state MTCM trellis for 32-SQ is shown in Figure 3.12 using the partitions of Figure 3.11. The simulation result is shown in Figure 3.10. As the simulation shows, the error performance for this scheme is worse than the error performance based on 4- and 8-state MTCM schemes based on 16-QAM. However, 32-SQ has a higher information rate at 4 information bits/symbol than 16-QAM at three information bits/symbol. A more appropriate comparison would be to normalize the E_b/N_o axis of Figure 3.10 by the information rate of each code or to compare the BER of the two codes. This is left to the reader.

The symbol error performance of the 16-state MTCM scheme based on 32-SQ compared to the error performance of the 8-state MTCM scheme may be estimated through equation 3.1. For the 16-state scheme, the minimum product of the squared Euclidean distance over the parallel path is equal to 640. This minimum product is equal to 64 for the 8-state scheme. The improvement in error performance is therefore

---

[4] This result was confirmed through simulations.

10log(340/64)=10 dB. This substantial improvement is a function of the partitioning of the composite signal set.

(0,0)(2,2)(18,18)(16,16)(9,9)(11,11)(27,27)(25,25)(1,19)(3,17)(19,1)(17,3)(8,26)(10,24)(26,8)(24,10) - A1
(6,6)(4,4)(20,20)(22,22)(15,15)(13,13)(29,29)(31,31)(7,21)(5,23)(21,7)(23,5)(14,28)(12,30)(28,14)(30,12)

(0,2)(2,18)(18,16)(16,0)(9,11)(11,27)(27,25)(25,9)(1,31)(3,15)(19,13)(17,29)(8,22)(10,6)(26,4)(24,20) - A2
(6,10)(4,26)(20,24)(22,8)(15,3)(13,19)(29,17)(31,1)(7,23)(5,7)(21,5)(23,21)(14,30)(12,14)(28,12)(30,28)

(0,4)(2,20)(18,22)(16,6)(9,13)(11,29)(27,31)(25,15)(1,25)(3,9)(19,11)(17,27)(8,16)(10,0)(26,2)(24,18) - A3
(6,12)(4,28)(20,30)(22,14)(15,5)(13,21)(29,23)(31,7)(7,17)(5,1)(21,3)(23,19)(14,24)(12,8)(28,10)(30,26)

(0,6)(2,4)(18,20)(16,22)(9,15)(11,13)(27,29)(25,31)(1,21)(3,23)(19,7)(17,5)(8,28)(10,30)(26,14)(24,12) - A4
(6,8)(4,10)(20,26)(22,24)(15,1)(13,3)(29,29)(31,17)(7,27)(5,25)(21,9)(23,11)(14,18)(12,16)(28,0)(30,2)

((0,8)(2,10)(18,26)(16,24)(9,1)(11,3)(27,19)(25,17)(1,27)(3,25)(19,9)(17,11)(8,18)(10,16)(26,0)(24,2) - A5
(6,14)(4,12)(20,28)(22,30)(15,7)(13,5)(29,21)(31,23)(7,29)(5,31)(21,15)(23,13)(14,20)(12,22)(28,6)(30,4)

(0,10)(2,26)(18,24)(16,8)(9,3)(11,19)(27,17)(25,1)(1,23)(3,7)(19,5)(17,21)(8,30)(10,14)(26,12)(24,28) - A6
(6,16)(4,0)(20,2)(22,18)(15,25)(13,9)(29,11)(31,27)(7,13)(5,29)(21,31)(23,15)(14,4)(12,20)(28,22)(30,6)

(0,12)(2,28)(18,30)(16,14)(9,5)(11,21)(27,23)(25,7)(1,17)(3,1)(19,3)(17,19)(8,24)(10,8)(26,10)(24,26) - A7
(6,22)(4,6)(20,4)(22,20)(15,31)(13,15)(29,13)(31,29)(7,11)(5,27)(21,25)(23,9)(14,2)(12,18)(28,16)(30,0)

(0,14)(2,12)(18,28)(16,30)(9,7)(11,5)(27,21)(25,23)(1,29)(3,31)(19,15)(17,13)(8,20)(10,22)(26,6)(24,4) - A8
(6,18)(4,16)(20,0)(22,2)(15,27)(13,25)(29,9)(31,11)(7,1)(5,3)(21,19)(23,17)(14,8)(12,10)(28,26)(30,24)

(0,16)(2,0)(18,2)(16,18)(9,25)(11,9)(27,11)(25,27)(1,13)(3,29)(19,31)(17,15)(8,4)(10,20)(26,22)(24,6) - A9
(6,24)(4,8)(20,10)(22,26)(15,17)(13,1)(29,3)(31,19)(7,5)(5,21)(21,23)(23,7)(14,12)(12,28)(28,30)(30,14)

(0,18)(2,16)(18,0)(16,2)(9,27)(11,25)(27,9)(25,11)(1,1)(3,3)(19,19)(17,17)(8,8)(10,10)(26,26)(24,24) - A10
(6,20)(4,22)(20,6)(22,4)(15,29)(13,31)(29,15)(31,13)(7,7)(5,5)(21,21)(23,32)(14,14)(12,12)(28,28)(30,30)

(0,20)(2,22)(18,6)(16,4)(9,29)(11,31)(27,15)(25,13)(1,7)(3,5)(19,21)(17,23)(8,14)(10,12)(26,28)(24,30) - A11
(6,26)(4,24)(20,8)(22,10)(15,19)(13,17)(29,1)(31,3)(7,9)(5,11)(21,27)(23,25)(14,0)(12,2)(28,18)(30,16)

(0,22)(2,6)(18,4)(16,20)(9,31)(11,15)(27,13)(25,29)(1,11)93,27)(19,25)(17,9)(8,2)(10,18)(26,16)(24,0) - A12
(6,30)(4,14)(20,12)(22,28)(15,23)(13,7)(29,5)(31,21)(7,3)(5,19)(21,17)(23,1)(14,10)(12,26)(28,24)(30,8)

(0,24)(2,8)(18,10)(16,26)(9,17)(11,1)(27,3)(25,19)(1,5)(3,21)(19,23)(17,7)(8,12)(10,28)(26,30)(24,14) - A13
(6,2)(4,18)(20,16)(22,0)(15,11)(13,27)(29,25)(31,9)(7,31)(5,15)(21,13)(23,29)(14,22)(12,6)(28,4)(30,20)

(0,26)(2,24)(18,8)(16,10)(9,19)(11,17)(27,1)(25,3)(1,9)(3,11)(19,27)(17,25)(8,0)(10,2)(26,18)(24,16) - A14
(6,28)(4,30)(20,14)(22,12)(15,21)(13,23)(29,7)(31,5)(7,15)(5,13)(21,19)(23,31)(14,6)(12,4)(28,20)(30,22)

(0,28)(2,30)(18,14)(16,12)(9,21)(11,23)(27,7)(25,5)(1,15)(3,13)919,29)(17,31)98,6)(10,4)(26,20)(24,22) - A15
(6,0)(4,2)(20,18)(22,16)(15,9)913,11)(29,27)(31,25)(7,19)(5,17)921,1)(23,3)(14,26)912,24)(28,8)(30,10)

(0,30)(2,14)918,12)(16,28)(9,23)(11,7)(27,5)(25,21)(1,3)(3,19)(19,17)(17,1)(8,10)(10,26)(26,24)(24,8) - A16
(6,4)(4,20)920,22)(22,6)(15,13)(13,29)(29,31)(31,15)(7,25)(5,9)(21,11)(23,27)(14,16)(12,0)(28,2)(30,18)

Figure 3.11 - Partitioning for 32-SQ with k=2

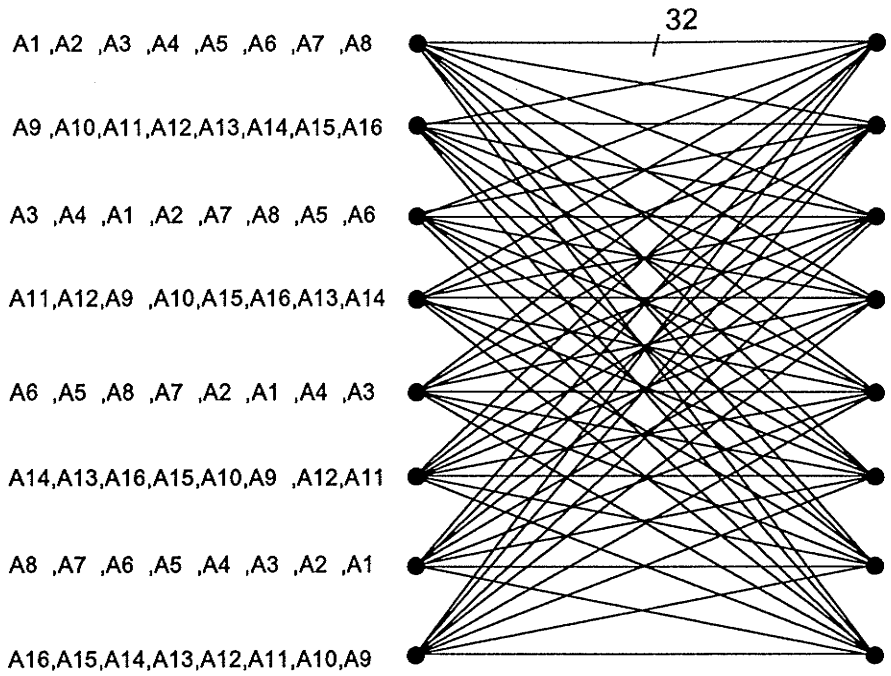

Figure 3.12 - 8-state trellis for MTCM scheme based on 32-SQ

3.4.6 - 64-QAM, multiplicity k=2

64-QAM is the largest signal set considered in this thesis. There are 4,096 composite symbols of which 2,048 are required for the scheme. Of the 1,024 composite symbols per node, no more than 64 may be in the highest partition in order to maintain a error event length of L=2. The minimum acceptable number of states in the trellis is 16. The highest level of partitioning must have 32 partitions, each with 64 composite symbols. This partitioning level is shown in Appendix A.

It was not possible to design an optimum MTCM scheme for this signal set due to the large number of states and composite symbols involved. Furthermore, it was not possible to estimate the performance of the scheme since equation 3.1 is not accurate in such a case.

3.4.7 - Processing time delays for various schemes

Figure 3.13 shows the relative processing time for the various MTCM schemes designed in this section. The processing times shown in figure 3.13 apply to the general purpose Viterbi decoder developed for this thesis. The nomenclature in Figure 3.13 is as follows: s2k2 refers to a 2-state trellis with multiplicity k=2; similarly, s8k1 refers to the optimum 8-state trellis with multiplicity k=1. Each bar in the graph identifies the number of states and the multiplicity of the scheme for specific signal sets. As expected, the relative processing time increases with the number of states in a trellis and the number of symbols in the signal set. For example, doubling the number of symbols in the signal set while maintaining the same number of states in a trellis quadruples the number of parallel paths. This in turn quadruples the number of computations and comparisons at each state in the Viterbi decoder. Doubling the number of states in a trellis while retaining the same signal set doubles the overall number of computations in the Viterbi decoder. Furthermore, the memory requirement doubles and more time is spent shifting data in memory.

Because the Viterbi decoder is required to handle a large variety of schemes, it is relatively inefficient. For example, the large number of memory manipulations results in poor performance when applied to schemes with large number of states. A more efficient implementation would reduce the amount of data shuffling in memory. Therefore, the results shown in this section should not be considered representative for a practical implementation. They are included only to allow the reader to get a general idea of the relative processing times for various schemes.

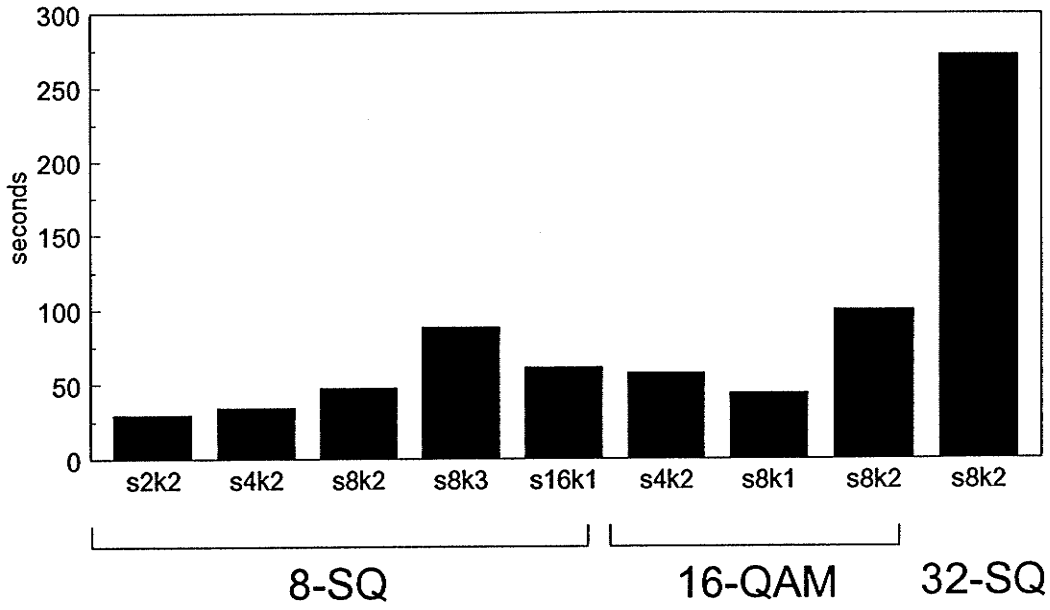

Figure 3.13 - Relative processing times for various schemes

3.5 - Increasing the multiplicity

All the MTCM schemes considered up to this point have a multiplicity of k=2. It is possible to use signal sets based on a greater multiplicity. This is equivalent to increasing the diversity of a scheme. In order to increase the performance of MTCM schemes over the Rayleigh fading channel by increasing the multiplicity and hence, the minimum error event length to L=k, the number of states in a trellis must also increase. For example, consider a 8-SQ signal set with a multiplicity of k=3. There are 8^3=512 composite symbols in this signal set and each composite symbol represents 6 information bits. Therefore, there must be 2^6=64 composite symbols at each node of the trellis. 128 composite symbols or one quarter of the available composite symbol set is required for the scheme. Furthermore, since there cannot be more than 8 parallel paths to maintain an error event length of L=3, there must be 64/8=8 states in the trellis. This scheme falls within the parameters established for this thesis and is described in section 3.5.1.

Increasing the multiplicity to k=4 with the same signal set would result in a trellis with at least 32 states. Similarly, using a multiplicity of k=3 and a M=16 signal set would also require a trellis with at least 32 states. Therefore, an increase in the multiplicity only results in trellises with less than 16 states for small signal sets with $M \leq 8$. The performance of optimum MTCM schemes based on 8-SQ and a multiplicity of k=3 is discussed below.

The performance of MTCM schemes based on 8-SQ and a multiplicity of k=3 is examined here as an example. The partitioning of 8-SQ for a multiplicity of k=3 is conducted using the same methodology as for a multiplicity of k=2. First, the 128 composite symbols are selected and paired at the lowest level of partitioning. For example, the composite symbol (0,0,0) is paired with its complement (5,5,5). The 64 pairs of composite symbols are partitioned into 32 partitions of 4 composite symbols each and then into 16 partitions of 8 composite symbols each. These sixteen partitions and the 8-state trellis are shown in figure 3.14.

Figure 3.15 compares the performance of this scheme with the performance of the 8-state MTCM scheme based on the same signal set but with a multiplicity of k=2. The error performance of the scheme based on a multiplicity of k=2 is superior to the error performance of the scheme based on a multiplicity of k=3. This is explained by comparing the two trellises. First, consider the trellis for the multiplicity of k=2 shown in figure 3.4. There are only two parallel paths and the pairs of composite symbols over the parallel paths are complements of each other. Therefore, the product of the squared Euclidean distance over the parallel paths is $32^2=1024$. Now consider the trellis for the multiplicity of k=3. There are 8 parallel paths and the product of the squared Euclidean distance over the parallel paths is $8^3=512$. Since the performance of both of these trellises is limited by the parallel paths, it follows that the error performance of the MTCM scheme based on a multiplicity of k=3 must be inferior to the performance of the MTCM scheme based on a multiplicity of k=2 even though the minimum error event length is smaller. Therefore, there are no advantages in increasing the multiplicity to k=3 for an

8-state trellis.

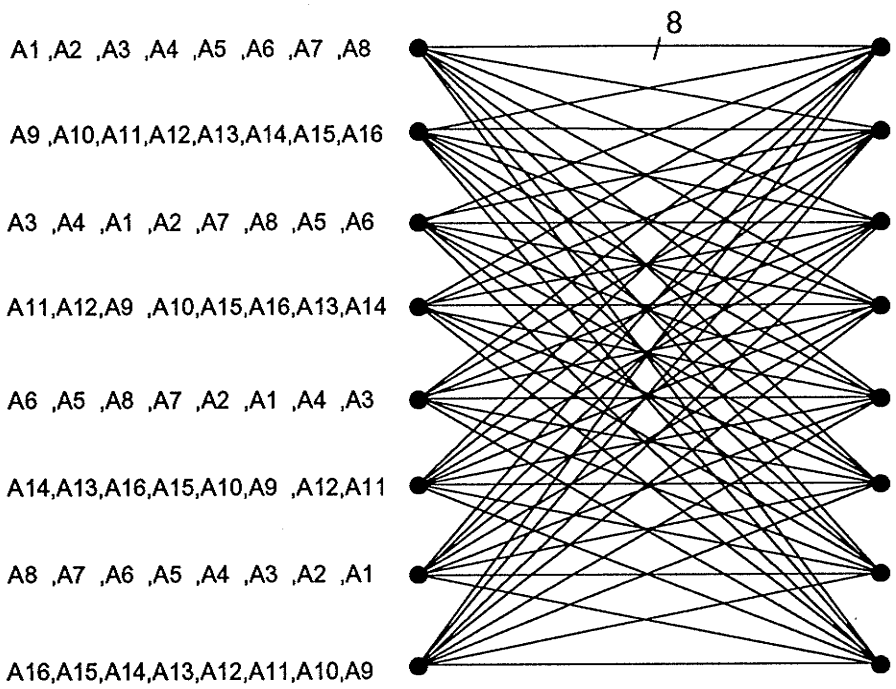

(0,0,0)(5,5,5)(1,1,1)(4,4,4)(2,2,2)(7,7,7)(3,3,3)(6,6,6) - A1
(0,0,1)(5,5,4)(1,1,5)(4,4,0)(2,2,6)(7,7,3)(3,3,2)(6,6,7) - A2
(0,0,5)(5,5,0)(1,1,4)(4,4,1)(2,2,7)(7,7,2)(3,3,6)(6,6,3) - A3
(0,0,4)(5,5,1)(1,1,0)(4,4,5)(2,2,3)(7,7,6)(3,3,7)(6,6,2) - A4
(0,1,0)(5,4,5)(1,5,1)(4,0,4)(2,6,2)(7,3,7)(3,2,3)(7,7,6) - A5
(0,1,1)(5,4,4)(1,5,5)(4,0,0)(2,2,6)(7,7,3)(3,3,2)(6,6,7) - A6
(0,1,5)(5,4,0)(1,5,4)(4,0,1)(2,6,7)(7,3,2)(3,2,6)(6,7,3) - A7
(0,1,4)(5,4,1)(1,5,0)(4,0,5)(2,6,3)(7,3,6)(3,2,7)(6,7,2) - A8
(0,5,0)(5,0,5)(1,4,1)(4,1,4)(2,7,2)(7,2,7)(3,6,3)(6,3,6) - A9
(0,5,1)(5,0,4)(1,4,5)(4,1,0)(2,7,6)(7,2,3)(3,6,2)(6,3,7) - A10
(0,5,5)(5,0,0)(1,4,4)(4,1,1)(2,7,7)(7,2,2)(3,6,6)(6,3,3) - A11
(0,5,4)(5,0,1)(1,4,0)(4,1,5)(2,7,3)(7,2,6)(3,6,7)(6,3,2) - A12
(0,4,0)(5,1,5)(1,0,1)(4,5,4)(2,3,2)(7,6,7)(3,7,3)(6,2,6) - A13
(0,4,1)(5,1,4)(1,0,5)(4,5,0)(2,3,6)(7,6,3)(3,7,2)96,27) - A14
(0,4,5)(5,1,0)(1,0,4)(4,5,1)(2,3,7)(7,6,2)(3,7,6)(6,2,3) - A15

Figure 3.14 - 8-state MTCM scheme based on 8-SQ with k=3

Now consider a 16-state trellis. The trellis for a multiplicity of k=2 will have no parallel path and the minimum error event length will be L=3. The trellis with the multiplicity of k=3 will have 4 parallel paths per branch and the error event length will also be 3. Since there are no parallel paths in the trellis based on a multiplicity of k=2, the product of the squared Euclidean distance over the minimum error event length for that

trellis is larger than for the trellis based on a multiplicity of k=3. Once again, there is no advantage in increasing the multiplicity to k=3 for a 16-state trellis.

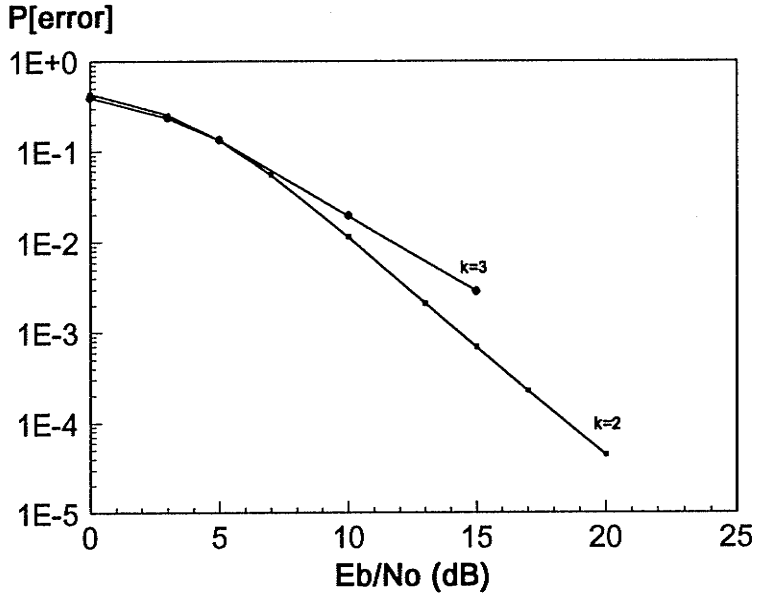

Figure 3.15 - P[error] in a Rayleigh fading channel for MTCM schemes based on 8-SQ with k=2 and k=3

3.6 - Summary

In order to design MTCM schemes for the Rayleigh fading channel, two design criteria must be met. The principal design criterion is the maximization of the length of the shortest error event. The second design criterion is the maximization of the product of the squared Euclidean distance over that error event. In order to satisfy the two design criteria, a method to partition a two-dimensional signal set was developed for two-dimensional signal sets that can be circumscribed by a square. It was shown that for these signal sets, the lower-level partitions are identical to the lower-level partitions obtained as if the scheme was designed for the AWGN channel. The higher-level partitions are obtained by using the reverse partitioning method described in Chapter 2.

To demonstrate this partitioning technique, 8-SQ, 8-QAM, 16-QAM, 32-SQ and 64-QAM signal sets based on a multiplicity of k=2 as well as 8-SQ based on a multiplicity of k=3 were partitioned. A number of optimum MTCM schemes for 2-, 4-, and 8-state trellises were designed for 8-SQ, 8-QAM, 16-QAM and 32-SQ signal sets. Unfortunately, optimum 16-state trellises could not be designed. However, the error performance of 16-state trellises based on these signal sets as well as 64-QAM was analyzed.

Through analyzing the error performance of various MTCM schemes, the following conclusions are made:

1. Increasing the number of states in a trellis always improves error performance. The amount of improvement depends on the signal set and is not always significant. The improvement comes at the expense of a longer decoding delay;

2. For signal sets with 8 symbols or less, there is no advantage in using MTCM for trellises with 16 or fewer states because TCM schemes based on the same signal set exhibit better error performance. For signal sets with more than 8 symbols, there is a definite advantage in using MTCM;

3. MTCM schemes based on a multiplicity of k=3 can only be designed to have less than 16 states if the signal set contains 8 symbols or less. Increasing the multiplicity of a MTCM scheme based on such a signal set from k=2 to k=3 does not result in an improvement in the error performance of the scheme for trellises with 16 or fewer states.

Chapter 4 - Component diversity

4.1 - General

This chapter examines a recent diversity technique developed by Giraud & al.[28,38]. Other diversity techniques have long been used to counter the effects of Rayleigh fading. Unfortunately, existing techniques are not well suited to commercial user-based mobile radio communication networks. For example, frequency diversity is costly in terms of bandwidth while space diversity, a technique that simultaneously uses multiple antennas, is not compatible with small handheld terminals. Consequently, Boulle and Belfiore's technique is better suited for mobile radio communication networks. Their technique will be referred to as component diversity.

Boulle and Belfiore developed component diversity for use with uncoded modulation schemes based on multidimensional signal sets. Section 4.2 reviews their work with an emphasis on two-dimensional signal sets. Component diversity may also be used in conjunction with TCM or MTCM schemes. The advantages and drawbacks of combining component diversity with other TCM and MTCM are discussed in Section 4.3.

4.2 - Component diversity

Figure 4.1 is a block diagram of a system using component diversity. Information bits are mapped to an individual symbol of a signal set Ω. A component interleaver is used to scramble the components of the transmitted symbols. At the receiver, the received symbols are component de-interleaved before maximum likelihood detection. The key to the performance of component diversity is the use of the component interleaver and de-interleaver. In addition, there is a restriction on the multidimensional signal set used to modulate the information bits. These two issues are discussed below.

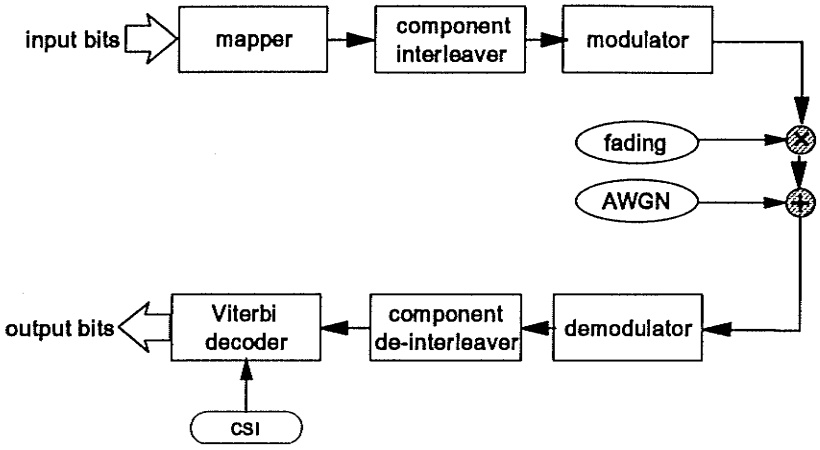

Figure 4.1 - Component diversity block diagram

The component interleaver is illustrated at Figure 4.2 for a two-dimensional signal set. Let $\mathbf{x}_1 \ldots \mathbf{x}_n$ denote n symbols with co-ordinates (x_{11},x_{12}) ... (x_{n1},x_{n2}). The two components of the n symbols are entered sequentially into the interleaver n symbols at a time. The symbols $\mathbf{y}_1 \ldots \mathbf{y}_n$ transmitted over the Rayleigh fading channel are composed of the two components each of the inputted $\mathbf{x}$ symbols For example, $\mathbf{y}_1=(x_{11}, x_{2n2})$. The transmitted symbols are therefore not the symbols to which the information bits were mapped, but "pseudo-symbols" generated by the component interleaver. At the de-interleaver, the original symbols are regenerated from the "pseudo-symbols". Because the two components of the original symbols were transmitted over the channel during different signalling intervals, they were subjected to different fading coefficients.

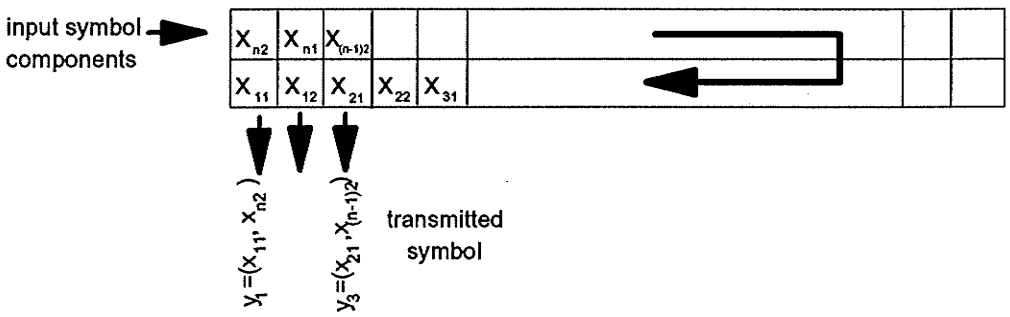

Figure 4.2 - Component interleaver

Assuming an infinite length interleaver, the fading coefficients for the two components of a symbol are uncorrelated. In this case, an upper bound on the asymptotic pairwise error probability is given in [28]

$$P(\tilde{x} \rightarrow x) \leq \left(\prod_{i=1}^{R} \frac{\Gamma E_s}{4N_0} |\tilde{x}_i - x_i|^2 \right)^{-1}$$

where $\frac{\Gamma E_s}{N_0}$ is the SNR.

The pairwise error probability decreases as the number of terms in the product increase, that is, as the number of distinct components between pairs of symbols in the signal set increases. Therefore, in order for component diversity to be effective, each symbol in the signal set must have unique components. Essentially, no two symbols in the signal set may share the same component. Furthermore, the distance between symbol components in any one dimension should be maximized. This is illustrated through the following example. Figure 4.3a is a 8-QAM signal set. Symbols 0 through 3 all share the same y-axis components. As such, this signal set is not useful for component diversity. Figure 4.3b illustrates the same 8-QAM signal set rotated by an angle $\phi = \pi/8$. Each symbol now has unique components in both axes and this signal set is more appropriate for component diversity. In general, there exists an angle ϕ , which any signal set may be rotated by, so that each symbol in the signal set has unique components and the distance between components is maximized. Appendix B demonstrates how to calculate the optimum rotation angle for various signal sets.

In the above example, it should be apparent that there are 64 possible pseudo-symbols transmitted while the original symbol set is composed of only 8 symbols. The average energy of the pseudo-signal set is the same as the energy of the original signal set. Figure 4.4 shows the P[error] for uncoded 8-QAM modulation over the Rayleigh fading channel using component diversity for angles of rotation ϕ equal to 0 and 22.5 degrees. The P[error] for normal uncoded 8-QAM modulation is also shown as a reference. As shown, component diversity does not lead to an improvement over

uncoded modulation if the signal set is not rotated. However, the combination of component diversity and an optimally rotated signal set results in a drastic improvement at large SNR.

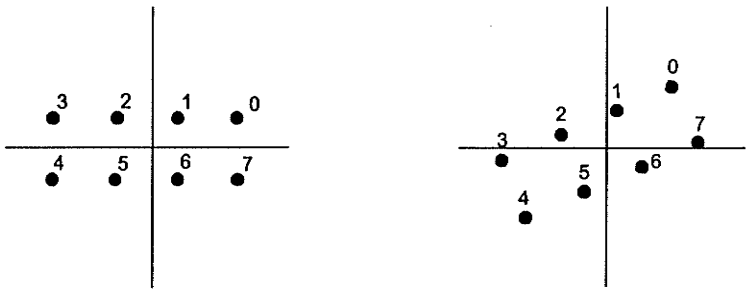

(a) (b)

Figure 4.3 - 8-QAM rotated by $\phi = \pi/8$

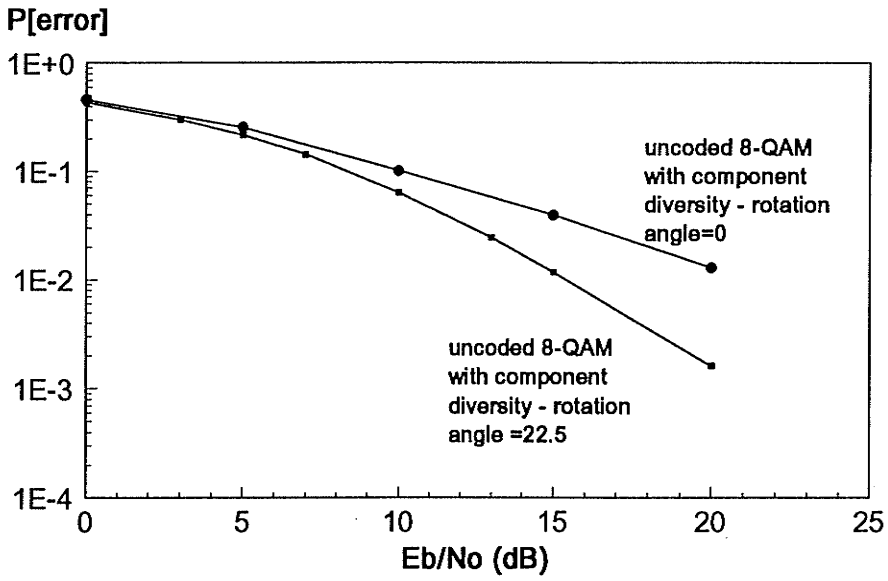

Figure 4.4 - P[error] in a Rayleigh fading channel for uncoded 8-QAM with component diversity and rotation angles of 0 and 22.5 degrees

As a last note, it must be mentioned that component interleaving requires memory in order to hold the fading coefficients for each signalling interval since there is a delay after the de-interleaving before the fading coefficients can be used for decoding. The amount of memory required increases with the length of the interleaver. Since correlation

between the fading coefficients of the two component of a symbol limits the performance of this technique, increases in memory correspond to increases in performance.

4.3 - Component diversity combined with MTCM

Component diversity may be combined with MTCM schemes designed for the Rayleigh fading channel to further improve their performance in a fading environment. Figure 4.5 illustrates a typical implementation. The component interleaving is performed after the information bits have been mapped to a sequence of symbols by the trellis encoder. The component de-interleaving is performed before the decoding. The fading coefficients for each component of each symbol in a sequence must be stored in memory until the individual symbols in the sequence are decoded through the Viterbi decoder. The use of memory is disadvantageous because of the increased complexity and cost of the receiver. However, this disadvantage may be offset by the increased error performance which results from combining component diversity and an MTCM scheme.

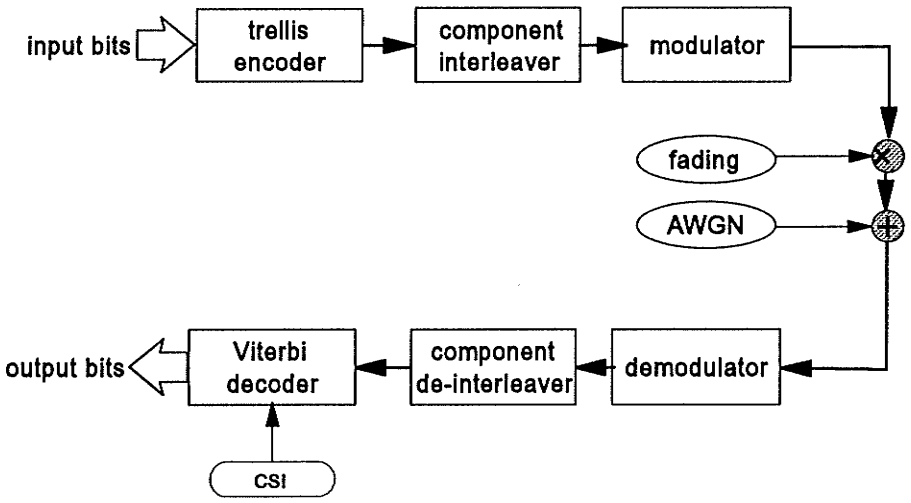

Figure 4.5 - MTCM and component diversity block diagram

This section presents simulated results from the combination of component diversity and two of the MTCM schemes from Chapter 3, namely 4-state 8-SQ and 16-QAM schemes. The results are presented at Figure 4.6. Also shown are the

performance of 4- and 8-state MTCM schemes based on 8-SQ and 16-QAM but without component diversity. It is apparent that the use of component diversity substantially increases the performance of both 4-state 8-SQ and 16-QAM schemes. Furthermore, the use of component diversity and 4-states MTCM schemes results in higher error performance than doubling the number of states of the MTCM schemes. In other words, the disadvantage of using more memory for component diversity is offset by the quicker decoding due to the smaller number of states in the trellis.

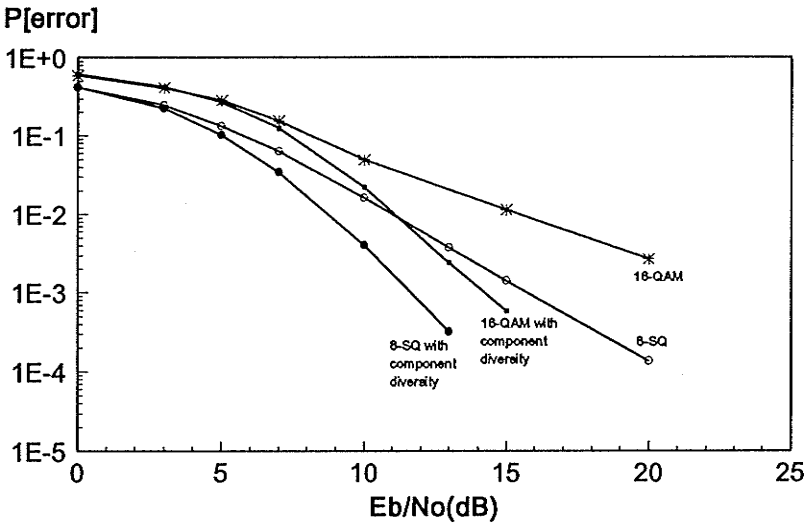

Figure 4.6 - P[error] in a Rayleigh fading channel for MTCM schemes with and without component diversity

4.4 - Summary

This chapter described a recent diversity technique known as component diversity. The advantages and disadvantages of using component diversity were examined. The main disadvantage of this technique is the requirement for memory to store the transmitted symbol component fading coefficients until they are needed for decoding.

The main advantage is the significant improvement in error performance for both uncoded modulation and MTCM schemes.

Chapter 5 - Concluding material

5.1 - Summary

This thesis designed and analyzed TCM and MTCM schemes based on M-QAM and similar two-dimensional signal constellations for the Rayleigh fading channel. This work was pursued in an effort to increase the channel capacity of mobile radio communication without increasing the bandwidth or power requirements. Although methods for designing TCM and MTCM schemes based on M-AM and M-PSK for the Rayleigh fading channel have already been developed, there was no method to design TCM and MTCM schemes based on two-dimensional signal sets. Two-dimensional signal sets have better distance properties than one-dimensional signal sets. As a result, they lead to better error performance for a given data rate especially for large signal constellations.

Chapter 2 reviewed the basic principles of TCM and MTCM for the AWGN channel. It was shown that the performance of a TCM or a MTCM scheme depends on how the symbols are mapped to the various paths in the trellis. For an optimum scheme, the signal set must be partitioned in such a way that the minimum squared Euclidean distance between symbols in each subset is maximized, regardless of the level of partitioning. In addition, these subsets must be mapped into the various branches in the trellis in such a way as to maximize the free distance of the trellis. The obvious method that partitions a composite signal set by dividing the composite symbols making up a partition into two new sub-partitions was found to be awkward for signal sets with 16 symbols or more. To handle larger composite signal sets, a new method referred to as the reverse partitioning method was devised. The reverse partitioning method proved to be relatively simple to implement and can be used to partition relatively large two-dimensional composite signal sets. The method assumes that the lower-level subsets are known. The lower-level subsets are then combined in increasingly large subsets at higher-levels of partitioning.

Chapter 3 began with an examination of the criteria for designing TCM and MTCM schemes for the Rayleigh fading channel. There are two criteria that must be met in order to design optimal TCM and MTCM schemes for the Rayleigh fading channel. The maximization of the length of the shortest error event is the principal design criterion. The maximization of the product of the squared Euclidean distance over that error event is the second design criterion. It was shown that MTCM schemes are required in order to satisfy both criteria for large signal sets. The problem of partitioning two-dimensional composite signal sets for MTCM while satisfying the two design criteria for the Rayleigh fading channel was then addressed. It was shown that for two-dimensional signal sets such as 8- and 32-SQ and 16- and 64-QAM which are circumscribed by a square, the lower-level of partitioning for the Rayleigh fading channel is the same as for the AWGN channel. Consequently, the reverse partitioning method developed in Chapter 2 can be applied. This result was used to design MTCM schemes based on two-dimensional composite signal sets and their error performance was analyzed. The effect of increasing the multiplicity from k=2 to k=3 was also investigated.

Chapter 4 examined component diversity. This technique is useful to improve the error performance of both uncoded and coded modulation schemes over the Rayleigh fading channel. It employs a component interleaver to ensure that each symbol components is affected by a different fading coefficient during transmission. For component diversity to be effective, a major restriction on the signal set must be satisfied. Each symbol in a signal set must have distinct components and the differences between the components must be maximized. It was shown that existing signal sets can be rotated by an optimal angle in order to satisfy this condition. The disadvantage of using component diversity is the requirement for additional memory to hold the symbol components fading coefficients until they are needed for decoding. Finally, the improvement in error performance of two MTCM schemes designed in Chapter 3 was examined for the case when these schemes are combined with component diversity.

5.2 - Conclusion

The work conducted for this thesis leads to the following conclusions:

1. The reverse partitioning method is useful to partition two-dimensional composite signal sets for MTCM. The method may be used for relatively large signal sets.

2. The optimum partitioning of two-dimensional composite signal sets that satisfy the two criteria for the Rayleigh fading channel may be performed using the reverse partitioning method if the signal set in question is circumscribed by a square.

3. For signal sets with 8 symbols or less, there is no advantage is using MTCM for trellises with 16 or fewer states because TCM schemes based on the same signal set exhibit better error performance over the Rayleigh fading channel. For signal sets with more than 8 symbols, there is a definite advantage in using MTCM over the Rayleigh fading channel.

4. Increasing the number of states in a trellis always improves error performance for a given signal set but results in a longer decoding delay.

5. MTCM schemes based on a multiplicity of k=3 may be designed to have less than 16 states only if the signal set contains 8 symbols or less. Increasing the multiplicity of a MTCM scheme based on such a signal set from k=2 to k=3 does not result in an improvement in the error performance of the scheme for trellises with 16 or fewer states.

6. Lastly, the examination of component diversity in terms of its usefulness concluded that the main advantage of this technique relates to the

significant improvement in error performance for both uncoded modulation and MTCM schemes. The main disadvantage relates to the requirement for memory to store the transmitted symbol component fading coefficients until they are needed for decoding.

5.3 - Proposal for future work

Three issues addressed in this thesis were left incomplete and deserve further attention.

1. This thesis only developed MTCM schemes with 8-state trellises. Designing optimum 16-state schemes is fairly complex. However, the gain in error performance of 16-state MTCM schemes compared to MTCM schemes with fewer trellis states may make the exercise worthwhile. The partitioning for a number of signal sets has already been done in this thesis and the results are directly applicable to MTCM schemes with 16-state trellises.

2. The only composite signal sets considered in this thesis, except for 8-QAM, are composite signal sets based on signals sets that can be circumscribed by a square. For these composite signal sets, the lower-level of partitioning is identical for the AWGN and the Rayleigh fading channel. As a result, the reverse partitioning method can be used. There may be other signal sets which are not circumscribed by a square but for which the lower-level of partitioning is the same for the AWGN and the Rayleigh fading channel. Some of these signal sets might have better distance properties than the signal sets considered in this thesis. MTCM schemes with better error performance could be designed based on these signal sets if such is the case.

3. The reverse partitioning method might also apply to signal sets circumscribed by a cube or hypercube for three and four dimensional signal sets respectively. It could be of interest to verify whether this is the case.

References

[1] A. Afrashteh, N.R. Sollenberger and D. Chukurov, "Signal to interference performance for a TDMA portable radio link," Proc. of the 41st Conf. on Veh Tech., pp. 204-208, May 1991.

[2] R. Agusti and G. Femenias, "Frequency-hopping trellis coded 8-DPSK for indoor communications," Proc. of the 41st Conf. on Veh Tech., pp. 211-215, May 1991.

[3] F. Amoreso, "The bandwidth of digital data signals," IEEE Commun. Mag., pp. 13-24, Nov 1980.

[4] E. Arthurs and H. Dym, "On the optimum detection of digital signals in the presence of white gaussian noise - a geometric interpretation of a study of three basic data transmission systems," IRE Trans. Commun. Syst., vol. CS-10, pp. 100-136, Dec 1962.

[5] F. Bacchus and P. Strickland, "Microstrip base station antennas for cellular communications," Proc. of the 41st Conf. on Veh Tech., pp. 166-171, May 1991.

[6] S. Benedetto, M. Mondin, G. Montorsi and L. Mallard, "Geometrically uniform multidimensional PSK trellis codes," Electronics Letters, vol. 28, pp. 1286-1288, Jul 1992.

[7] E. Biglieri, D. Divsalar, P. McLane. and M. Simon, Introduction to Trellis-Coded Modulation with Applications, New York: MacMillan, 1991.

[8] R. Blahut, Theory and Practice of Error Control Codes, Reading: Addison-Wesley, 1984.

[9] A.R. Calderbank and N.J.A. Sloane, "New trellis codes based on lattices and cosets," IEEE Trans. Inform. Theory, vol. IT-33, pp. 177-195, Mar 1987.

[10] J.K. Cavers "Variable-rate transmission for Rayleigh fading channels," IEEE Trans. Commun. Vol. 20, pp. 15-22, Feb 1972.

[11] J.K. Cavers, "An analysis of pilot symbol assisted 16-QAM for digital mobile communications," Proc. of the 41st Conf. on Veh Tech., pp. 380-385, May 1991.

[12] J.K. Cavers and P. Ho, "Analysis of the error perfromance of trellis-coded modulation in Rayleigh fading channels," IEEE Trans. Commun., vol. 40, pp.74-83, Jan 1992.

[13] KY. Chan and A. Bateman, "The performance of reference-based M-ary PSK with trellis coded modulation in Rayleigh fading," IEEE Trans. Veh. Tech., vol. 41, pp. 190-198, May 1992.

[14] Daniel Costello, "Coding techniques - introduction," IEEE Trans. Inform. Theory, vol IT-34, pp. 1122-1151, Sep 1988.

[15] L.W. Couch, Digital and Analog Communication Systems, New York: Macmillan, 1993.

[16] F. Davarian, "Mobile digital communications via tone calibration," IEEE Trans. Veh. Tech, vol. VT-36, pp.55-62, May 1987.

[17] D. Divsalar and M. Simon, "Combined trellis coding with asymmetric modulations," in the Conf. Record GlobeCom 1985, pp. 21.2.1-21.2.7, Dec 1985.

[18] D. Divsalar and M. Simon, "Multiple trellis coded modulation (MTCM)," IEEE Trans. Commun., vol. 36, pp. 410-419, Apr 1988.

[19] D. Divsalar and M. Simon, "The design of trellis coded MPSK for fading channels: performance criteria," IEEE Trans. Commun., vol. 36, pp. 1004-1011, Sep 1988.

[20] D. Divsalar and M. Simon, "The design of trellis coded MPSK for fading channels: set partitioning for optimum code design," IEEE Trans. Commun, vol. 36, pp. 1013-1021, Sep 1988.

[21] D. Divsalar and M. Simon, "Generalized multiple trellis coded modulation (MTCM)," in the Conf. Record GlobeCom 1987, pp. 20.3.1-20.3.7, Nov 1987.

[22] D. Divsalar and M. Simon, "Trellis coded modulation for 4800-9600 bits/s transmission over a fading mobile satellite channel," IEEE J. Sel. Areas in Commun., vol. SAC-5, pp. 162-174, Feb 1987.

[23] D. Divsalar and K. Simon, "Multiple symbol differential detection of MPSK," IEEE Trans. Commun., vol. 38, pp. 300-305, Mar 1990.

[24] D. Divsalar, K. Simon, T. Jedrey, N. Lay and W. Rafferty, "Combined trellis coding and feedforward processing for MSS applications," Proc. of the Second International Mobile Satellite Conf. IMSC 90, pp. 175-181, Jun 1990.

[25] D. Forney, Jr., "The Viterbi algorithm," IEEE Proc., vol. 61, pp. 268-278, Feb 1973.

[26] D. Forney, Jr., "Coset codes - part I: introduction and geometrical classification," IEEE Trans. on Inform. Theory, vol. IT-34, pp. 1123-1151, Sep 1988.

[27] A. Fung and P. McLane, "Phase jitter sensitivity of rotationally invariant 8 and 16 point trellis codes," IEE Proc., vol. 138, pp. 247-255, Aug 1991.

[28] X. Giraud, K. Boulle, JC Belfiore and U. Dropmann. "Constellations designed for the Rayleigh fading channel," Departement des communications de france, ecole nationale superieure des telecommunications, unpublished report.

[29] S. Heerelall, "Long term spectrum requirements for land mobile communications in Canada," Proc. of the 41st Conf. on Veh Tech., pp. 720-724, May 1991.

[30] M. Ikura, K. Ohno, Y. Yamao and F. Adachi, "Field experiments on TDMA mobile radio transmissions," Proc. of the 41st Conf. on Veh Tech., pp. 669-674, May 1991.

[31] G. Irvine and P. McLane. "Symbol-aided plus decision-directed reception for PSK/TCM modulation on shadowed mobile satellite fading channels," IEEE J. Sel. Areas in Commun., vol. SAC-10, pp. 1289-1299, Oct 1992.

[32] W. Jakes, Microwave Mobile Communications, New York: John Wiley & Sons, 1974.

[33] M.C. Jeruchim, "Techniques for estimating the bit error rate in the simulation of digital communication systems," IEEE J. Sel. Areas in Commun., Vol. SAC-2, pp. 153-161, Jan 1984.

[34] K. Kinoshita, M. Kuramoto, and N. Nakijama, "Development of a TDMA digital cellular system based on Japanese standard," Proc. of the 41st Conf. on Veh Tech., pp. 642-645, May 1991.

[35] S. Kwa, M. Vanderaar, J. Kim and G. Stevens, "Performance evaluation of land mobile satellite system under fading and interference using multiple TCM by Monte-Carlo simulation," Conf. Record GlobeCom 1991, pp. 43.6.1-43.6.5., Dec 1991.

[36] W. Lee, Mobile Communications Engineering, New York: McGraw-Hill, 1982.

[37] W. Lee, Mobile Cellular Communication Systems, New York: McGraw-Hill, 1989.

[38] Leeuwin-Boulle, and Belfiore, "Modulation schemes designed for the Rayleigh channel," Conf. Record 1991 Symp. Inform. Theory and Applications (SITA 91), Dec 1991.

[39] Shu Lin, "Multi-dimensional modulation codes for fading channels," Technical Report to NASA Goddard Space Flight Center (NASA 91-003), Oct 1991.

[40] S. Lin and D. Costello Jr., Error Control Coding: Fundamentals and Applications, Inglewood Cliffs: Prentice Hall, 1983.

[41] S. McCann, "Mobile data communications," Proc. of the 41st Conf. on Veh Tech., pp. 94-97, May 1991.

[42] J.P. McGrehan and A.J. Bateman, "Phase-locked transparent tone-in-band (TTIB): a new spectrum configuration particularly suited to the transmission of data over SSB mobile radio networks," IEEE Trans. on Commun., vol COM-32, pp. 81-87, Jan 1984.

[43] P. McLane, P. Wittke, P. Ho,and C. Loo, "PSK and DPSK trellis codes for fast fading, shadowed mobile satellite communications channels," IEEE Trans. on Commun., Vol. 36, pp. 1242-1246, Nov 1988.

[44] R. McKay, P. McLane and E. Biglieri, "Analytical performance bounds on average bit error probability for trellis coded PSK transmitted over fading channels," Conf. record of GlobeCom1989, pp. 9.2.1-9.2.7., Nov 1989.

[45] S. Massoumi and S. Kallel, "Adaptive trellis coded modulation for mobile communications," Conf. Record of the IEEE Pacific Rim Conf. on Commun, Comp. and Sig. Processing, pp. 538-541, May 1991.

[46] M. Moher and J. Lodge, "Performance of concatenated Reed-Solomon trellis-coded modulation over Rician fading channels," Proc. of the Second International Mobile Satellite Conf. IMSC 90, pp. 600-604, Jun 1990.

[47] J. Pieper, J. Proakis, R. Reed and J. Wolf, "Design of efficient coding and modulation for a Rayleigh fading channel," IEEE Trans. Inform. Theory, Vol IT-24, pp. 457-468, Jul 1974.

[48] S. Sampei and T Suraga, "Rayleigh compensation for QAM in land mobile radio communications," IEEE Trans. on Veh. Techno., Vol. 42, pp. 137-146, May 1993.

[49] S. Sampei and T Suraga, "Rayleigh fading compensation method for 16QAM in digital land mobile radio channels," Proc. of the IEEE Veh. Technology Conf., pp 640-646, May 1989.

[50] E.J. Schimmel, "Spectrum outlook in the United States," Proc. of the 41st Conf. on Veh Tech., pp. 716-719, May 1991.

[51] H.P Stern, "Compression techniques for mobile data terminal communication," Proc. of the 41st Conf. on Veh Tech., pp. 429-432, May 1991.

[52] C. Tellamburer, Q. Wang and V. Bhargava, "A performance analysis of trellis-coded modulation schemes over Rician fading channels," IEEE Trans. Veh. Tech., vol. 42, pp. 491-501, Nov 1993.

[53] G. Ungerboeck, "Trellis-coded modulation with redundant signal sets part I: introduction," IEEE Commun. Mag., Vol. 25, pp. 5-11, Feb 1987.

[54] G. Ungerboeck, "Trellis-coded modulation with redundant signal sets part II: state of the art," IEEE Commun. Mag., vol. 25, pp. 12-21, Feb 1987.

[55] G. Ungerboeck, "Channel coding with multilevel/phase signals," IEEE Trans. on Inform. Theory, vol IT-28, pp. 55-67, Jan 1982.

[56] G. Ungerboeck and I. Csajka, "On improving data-link performance by increasing the channel alphabet and introducing sequence coding," 1976 Int. Symp. Inform. Theory, Ronneby, Sweden, Jun 1976.

[57] A. J. Viterbi, "Error bounds for convolutional codes and an asymptotically optimum decoding algorithm," IEEE Trans. Inform. Theory, vol. IT-13, pp. 260-269, Apr 1967.

[58] A. Viterbi, J. Wolf, E. Zehavi, and R. Padovani, "A pragmatic approach to trellis-coded modulation," IEEE Commun. Mag., pp. 11-19, Jul 1989.

[59] H.B. Voelckner, "Phase-shift keying in fading channel," Proc. IEE, vol. 107, pp. 231-235, Jan 1960.

[60] W. Webb, L. Hanzo, R. Salami and R. Steele, "Does 16-QAM provide an alternative to a half-rate GSM speech codec?," Proc. of the 41st Conf. on Veh Tech., pp. 511-516, May 1991.

[61] S.G. Wilson, "Rate 5/6 trellis-code 8-PSK,, IEEE Trans. Commun., vol. COM-34, pp. 1045-1049, Oct 1986.

[62] J. Wolf and G. Ungerboeck, "Trellis coding for partial-response channels," IEEE Trans. Commun., vol. 34, pp. 765-772, August 1986.

[63] L. Wong and P. McLane, "Performance of trellis codes for a class of equalized ISI channels," IEEE Trans on Commun., vol 36, pp.1330-1336, Dec 1989.

[64] W. Wu, D. Haccoun, R. Peile and Y Hirata, "Coding for satellite communications," IEEE J. on Sel. Areas in Commun., vol SAC-5, pp. 724-748, May 1987.

[65] E. Zehavi, "8-PSK trellis codes for a Rayleigh channel," IEEE Trans. on Commun., vol. 40, pp. 873-884, May 1992.

Appendix A - Partitioning for 64-QAM

The 64-QAM signal set is shown at Figure A.1. Figure A.2 shows the partitioning for 64-QAM with multiplicity of k=2. There are 32 partitions of 64 composite symbols each. This partitioning is relevant to a MTCM scheme based on a trellis with 16 states. For schemes based on larger trellises, the partitions in Figure A.2 must be sub-partitioned into subsets with fewer composite symbols. The composite symbols in Figure A.2 have been arranged so that the sub-partitioning is evident. The sub-partitioning is done as follows.

First, consider the partitioning of the composite symbol set into 64 partitions of 32 composite symbols each. In this case, each partition in Figure A.2 must be divided into two subsets. One of the subset contains the first 32 composite symbols shown while the second subset contains the last 32 composite symbols. In turn, both subsets can be further partitioned into two sub-subsets each. Again, the first half of the composite symbols in a subset form one of the sub-subset. The last half of the composite symbols form the other sub-subset. The same pattern applies at each level of partitioning.

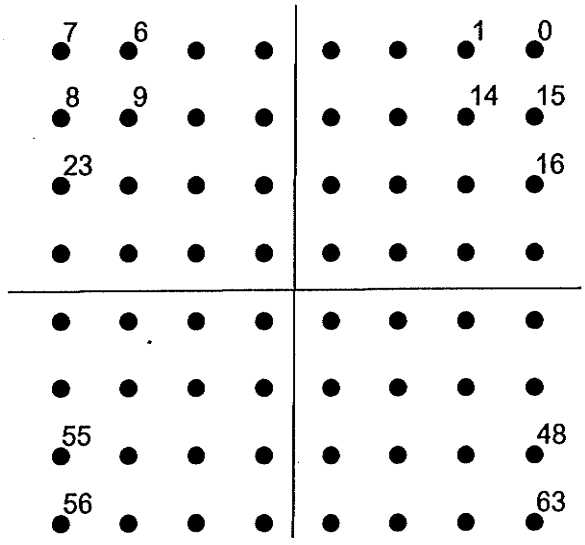

Figure A.1 - 64-QAM signal set

(0, 0)(4, 4)(36,36)(32,32)(2,38)(6,34)(38,2)(34,6)(16,52)(20,48)(52,16)(48,20)
(18,18)(22,22)(54,54)(50,50) (13,15)(9,11)(41,43)(45,47)(15,41)(11,45)(43,13)
(47, 9)(29,59)(25,63)(57,31) (61,27)(31,29)(27,25)(59,57)(63,61)(12,30)(8,26)
(40,58)(44,62)(14,56)(10,60)(42,28)(46,24) (28,42)(24,46)(56,14)(60,10)(30,12)
(26,8)(58,40)(62,44) (1,17)(5,21)(37,53)(33,49)(3,55)(7,51)(39,19)(35,23)
(17,37)(21,33)(53, 1)(49, 5)(19, 3)(23, 7)(55,39)(51,35)

(0, 2)(4, 6)(36,38)(32,34)(2,36)(6,32)(38,0)(34,4)(16,54)(20,50)(52,18)(48,22)
(18,16)(22,20) (54,52)(50,48) (13,13)(9,9)(41,41)(45,45)(15,43)(11,47)(43,15)
(47,11)(29,57)(25,61)(57,29) (61,25)(31,31)(27,27)(59,59)(63,63) (12,28)(8,24)
(40,56)(44,60)(14,58)(10,62)(42,30)(46,26) (28,40)(24,44)(56,12)(60,8)(30,14)
(26,10)(58,42)(62,46) (1,19)(5,23)(37,55)(33,51)(3,53)(7,49)(39,17)(35,21)
(17,39)(21,35)(53, 3)(49, 7)(19, 1)(23, 5)(55,37)(51,33)

(0, 4)(4,36)(36,32)(32, 0)(2,48)(6,16)(38,20)(34,52)(16,34)(20,2)(52,6)(48,38)
(18,22)(22,54) (54,50)(50,18) (13, 5)(9,37)(41,33)(45,1)(15,49)(11,17)(43,21)
(47,53)(29,35)(25,3)(57,7) (61,39)(31,23)(27,55)(59,51)(63,19) (12,20)(8,52)
(40,48)(44,16)(14,32)(10, 0)(42, 4)(46,36) (28,50)(24,18)(56,22)(60,54)(30, 6)
(26,38)(58,34)(62, 2) (1,21)(5,53)(37,49)(33,17)(3,33)(7, 1)(39, 5)(35,37)
(17,51)(21,19)(53,23)(49,55)(19, 7)(23,39)(55,35)(51, 3)

(0, 6)(4,38)(36,34)(32, 2)(2,50)(6,18)(38,22)(34,54)(16,32)(20,0)(52,4)(48,36)
(18,20)(22,52) (54,48)(50,16) (13, 7)(9,39)(41,35)(45, 3)(15,51)(11,19)(43,23)
(47,55)(29,33)(25, 1)(57,5) (61,37)(31,21)(27,53)(59,49)(63,17) (12,22)(8,54)
(40,50)(44,18)(14,34)(10, 2)(42, 6)(46,38) (28,48)(24,16)(56,20)(60,52)(30, 4)
(26,36)(58,32)(62, 0) (1,23)(5,55)(37,51)(33,19)(3,35)(7, 3)(39, 7)(35,39)
(17,49)(21,17)(53,21)(49,53)(19, 5)(23,37)(55,33)(51, 1)

(0, 8)(4,40)(36,44)(32,12)(2,60)(6,28)(38,24)(34,56)(16,46)(20,14)(52,10)(48,42)
(22,58)(18,26)(54,62)(50,30) (13, 9)(9,41)(41,45)(45,13)(15,61)(11,29)(43,25)
(47,57)(29,47)(25,15)(57,11)(61,43)(31,27)(27,59)(59,63)(63,31) (12,24)(8,56)
(40,60)(44,28)(14,44)(10,12)(42, 8)(46,40)(28,62)(24,30)(56,26)(60,58)(30,10)
(26,42)(58,46)(62,14) (1,25)(5,57)(37,61)(33,29)(3,45)(7,13)(39, 9)(35,41)
(17,63)(21,31)(53,27)(49,59)(19,11)(23,43)(55,47)(51,15)

(0,10)(4,42)(36,46)(32,14)(2,62)(6,30)(38,26)(34,58) (16,44)(20,12)(52,8)(48,40)
(18,24)(22,56)(54,60)(50,28) (13,11)(9,43)(41,47)(45,15)(15,63)(11,31)(43,27)
(47,59)(29,45)(25,13)(57, 9)(61,41)(31,25)(27,57)(59,61)(63,29) (12,26)(8,58)
(40,62)(44,30)(14,46)(10,14)(42,10)(46,42) (28,60)(24,28)(56,24)(60,56)(30,8)
(26,40)(58,44)(62,12) (1,27)(5,59)(37,63)(33,31)(3,47)(7,15)(39,11)(35,43)
(17,61)(21,29)(53,25)(49,57)(19, 9)(23,41)(55,45)(51,13)

(0,12)(4, 8)(36,40)(32,44)(2,42)(6,46)(38,14)(34,10)(16,56)(20,60)(52,28)(48,24)
(18,30)(22,26)(54,58)(50,62) (13, 3)(9, 7)(41,39)(45,35)(15,37)(11,33)(43, 1)
(47,5)(29,55)(25,51)(57,19)(61,23)(31,17)(27,21)(59,53)(63,49) (12,14)(8,10)
(40,42)(44,46)(14,40)(10,44)(42,12)(46, 8)(28,58)(24,62)(56,30)(60,26)(30,28)
(26,24)(58,56)(62,60) (1, 1)(5, 5)(37,37)(33,33)(3,39)(7,35)(39, 3)(35, 7)
(17,53)(21,49)(53,17)(49,21)(19,19)(23,23)(55,55)(51,51)

(0,14)(4,10)(36,42)(32,46)(2,40)(6,44)(38,12)(34, 8)(16,58)(20,62)(52,30)(48,26)
(18,28)(22,24)(54,56)(50,60) (13, 1)(9, 5)(41,37)(45,33)(15,39)(11,35)(43, 3)
(47, 7)(29,53)(25,49)(57,17)(61,21)(31,19)(27,23)(59,55)(63,51) (12,12)(8, 8)
(40,40)(44,44)(14,42)(10,46)(42,14)(46,10)(28,56)(24,60)(56,28)(60,24)(30,30)
(26,26)(58,58)(62,62) (1, 3)(5, 7)(37,39)(33,35)(3,37)(7,33)(39, 1)(35, 5)
(17,55)(21,51)(53,19)(49,23)(19,17)(23,21)(55,53)(51,49)

(0,16)(4,20)(36,52)(32,48)(2,54)(6,50)(38,18)(34,22) (16,36)(20,32)(52, 0)(48, 4)
(18, 2)(22, 6)(54,38)(50,34) (13,31)(9,27)(41,59)(45,63)(15,57)(11,61)(43,29)
(47,25) (29,43)(25,47)(57,15)(61,11)(31,13)(27, 9)(59,41)(63,45) (12,18)(8,22)
(40,54)(44,50)(14,52)(10,48)(42,16)(46,20) (28,38)(24,34)(56, 2)(60, 6)(30, 0)
(26, 4)(58,36)(62,32) (1,29)(5,25)(37,57)(33,61)(3,59)(7,63)(39,31)(35,27)
(17,41)(21,45)(53,13)(49, 9)(19,15)(23,11)(55,43)(51,47)

(0,18)(4,22)(36,54)(32,50)(2,52)(6,48)(38,16)(34,20) (16,38)(20,34)(52, 2)(48, 6)
(18, 0)(22, 4)(54,36)(50,32) (13,29)(9,25)(41,57)(45,61)(15,59)(11,63)(43,31)
(47,27) (29,41)(25,45)(57,13)(61, 9)(31,15)(27,11)(59,43)(63,47) (12,16)(8,20)
(40,52)(44,48)(14,54)(10,50)(42,18)(46,22) (28,36)(24,32)(56, 0)(60, 4)(30, 2)
(26, 6)(58,38)(62,34) (1,31)(5,27)(37,59)(33,63)(3,57)(7,61)(39,29)(35,25)
(17,43)(21,47)(53,15)(49,11)(19,13)(23, 9)(55,41)(51,45)

(0,20)(4,52)(36,48)(32,16)(2,32)(6, 0)(38, 4)(34,36) (16,50)(20,18)(52,22)(48,54)
(18, 6)(22,38)(54,34)(50, 2) (13,21)(9,53)(41,49)(45,17)(15,33)(11, 1)(43, 5)
(47,37) (29,51)(25,19)(57,23)(61,55)(31, 7)(27,39)(59,35)(63, 3) (12, 4)(8,36)
(40,32)(44, 0)(14,48)(10,16)(42,20)(46,52) (28,34)(24, 2)(56,6)(60,38)(30,22)
(26,54)(58,50)(62,18) (1, 5)(5,37)(37,33)(33, 1)(3,49)(7,17)(39,21)(35,53)
(17,35)(21, 3)(53, 7)(49,39)(19,23)(23,55)(55,51)(51,19)

(0,22)(4,54)(36,50)(32,18)(2,34)(6, 2)(38, 6)(34,38) (16,48)(20,16)(52,20)(48,52)
(18, 4)(22,36)(54,32)(50, 0) (13,23)(9,55)(41,51)(45,19)(15,35)(11, 3)(43, 7)
(47,39) (29,49)(25,17)(57,21)(61,53)(31, 5)(27,37)(59,33)(63, 1) (12, 6)(8,38)
(40,34)(44, 2)(14,50)(10,18)(42,22)(46,54) (28,32)(24, 0)(56,4)(60,36)(30,20)
(26,52)(58,48)(62,16) (1, 7)(5,39)(37,35)(33, 3)(3,51)(7,19)(39,23)(35,55)
(17,33)(21, 1)(53, 5)(49,37)(19,21)(23,53)(55,49)(51,17)

(0,24)(4,56)(36,60)(32,28)(2,44)(6,12)(38, 8)(34,40)(16,62)(20,30)(52,26)(48,58)
(18,10)(22,42)(54,46)(50,14) (13,25)(9,57)(41,61)(45,29)(15,45)(11,13)(43, 9)
(47,41) (29,63)(25,31)(57,27)(61,59)(31,11)(27,43)(59,47)(63,15) (12, 8)(8,40)
(40,44)(44,12)(14,60)(10,28)(42,24)(46,56)(28,46)(24,14)(56,10)(60,42)(30,26)
(26,58)(58,62)(62,30) (1, 9)(5,41)(37,45)(33,13)(3,61)(7,29)(39,25)(35,57)
(17,47)(21,15)(53,11)(49,43)(19,27)(23,59)(55,63)(51,31)

(0,26)(4,58)(36,62)(32,30)(2,46)(6,14)(38,10)(34,42)(16,60)(20,28)(52,24)(48,56)
(18, 8)(22,40)(54,44)(50,12) (13,27)(9,59)(41,63)(45,31)(15,47)(11,15)(43,11)
(47,43) (29,61)(25,29)(57,25)(61,57)(31, 9)(27,41)(59,45)(63,13) (12,10)(8,42)
(40,46)(44,14)(14,62)(10,30)(42,26)(46,58) (28,44)(24,12)(56,8)(60,40)(30,24)
(26,56)(58,60)(62,28) (1,11)(5,43)(37,47)(33,15)(3,63)(7,31)(39,27)(35,59)
(17,45)(21,13)(53, 9)(49,41)(19,25)(23,57)(55,61)(51,29)

(0,28)(4,24)(36,56)(32,60)(2,58)(6,62)(38,30)(34,26) (16,40)(20,44)(52,12)(48,8)
(18,14)(22,10)(54,42)(50,46) (13,19)(9,23)(41,55)(45,51)(15,53)(11,49)(43,17)
(47,21) (29,39)(25,35)(57, 3)(61, 7)(31, 1)(27, 5)(59,37)(63,33) (12, 2)(8,6)
(40,38)(44,34)(14,36)(10,32)(42, 0)(46, 4)(28,54)(24,50)(56,18)(60,22)(30,16)
(26,20)(58,52)(62,48) (1,13)(5, 9)(37,41)(33,45)(3,43)(7,47)(39,15)(35,11)
(17,57)(21,61)(53,29)(49,25)(19,31)(23,27)(55,59)(51,63)

(0,30)(4,26)(36,58)(32,62)(2,56)(6,60)(38,28)(34,24)(16,42)(20,46)(52,14)(48,10)
(18,12)(22, 8)(54,40)(50,44) (13,17)(9,21)(41,53)(45,49)(15,55)(11,51)(43,19)
(47,23) (29,37)(25,33)(57, 1)(61, 5)(31, 3)(27, 7)(59,39)(63,35) (12, 0)(8,4)
(40,36)(44,32)(14,38)(10,34)(42, 2)(46, 6)(28,52)(24,48)(56,16)(60,20)(30,18)
(26,22)(58,54)(62,50) (1,15)(5,11)(37,43)(33,47)(3,41)(7,45)(39,13)(35, 9)
(17,59)(21,63)(53,31)(49,27)(19,29)(23,25)(55,57)(51,61)

(0,32)(4, 0)(36, 4)(32,36)(2,20)(6,52)(38,48)(34,16) (16, 6)(20,38)(52,34)(48,2)
(18,50)(22,18)(54,22)(50,54) (13,33)(9, 1)(41, 5)(45,37)(15,21)(11,53)(43,49)
(47,17) (29, 7)(25,39)(57,35)(61, 3)(31,51)(27,19)(59,23)(63,55) (12,44)(8,12)
(40, 8)(44,40)(14,24)(10,56)(42,60)(46,28)(28,10)(24,42)(56,46)(60,14)(30,62)
(26,30)(58,26)(62,58) (1,45)(5,13)(37, 9)(33,41)(3,25)(7,57)(39,61)(35,29)
(17,11)(21,43)(53,47)(49,15)(19,63)(23,31)(55,27)(51,59)

(0,34)(4, 2)(36, 6)(32,38)(2,22)(6,54)(38,50)(34,18) (16, 4)(20,36)(52,32)(48,0)
(18,48)(22,16)(54,20)(50,52) (13,35)(9, 3)(41, 7)(45,39)(15,23)(11,55)(43,51)
(47,19) (29, 5)(25,37)(57,33)(6İ, 1)(31,49)(27,17)(59,21)(63,53) (12,46)(8,14)
(40,10)(44,42)(14,26)(10,58)(42,62)(46,30) (28,8)(24,40)(56,44)(60,12)(30,60)
(26,28)(58,24)(62,56) (1,47)(5,15)(37,11)(33,43)(3,27)(7,59)(39,63)(35,31)
(17, 9)(21,41)(53,45)(49,13)(19,61)(23,29)(55,25)(51,57)

(0,36)(4,32)(36, 0)(32, 4)(2, 2)(6, 6)(38,38)(34,34)(16,16)(20,20)(52,52)(48,48)
(18,54)(22,50)(54,18)(50,22) (13,37)(9,33)(41, 1)(45, 5)(15, 3)(11, 7)(43,39)
(47,35) (29,17)(25,21)(57,53)(61,49)(31,55)(27,51)(59,19)(63,23) (12,40)(8,44)
(40,12)(44, 8)(14,14)(10,10)(42,42)(46,46)(28,28)(24,24)(56,56)(60,60)(30,58)
(26,62)(58,30)(62,26) (1,41)(5,45)(37,13)(33, 9)(3,15)(7,11)(39,43)(35,47)
(17,29)(21,25)(53,57)(49,61)(19,59)(23,63)(55,31)(51,27)

(0,38)(4,34)(36, 2)(32, 6)(2, 0)(6, 4)(38,36)(34,32)(16,18)(20,22)(52,54)(48,50)
(18,52)(22,48)(54,16)(50,20) (13,39)(9,35)(41, 3)(45, 7)(15, 1)(11, 5)(43,37)
(47,33) (29,19)(25,23)(57,55)(61,51)(31,53)(27,49)(59,17)(63,21) (12,42)(8,46)
(40,14)(44,10)(14,12)(10, 8)(42,40)(46,44)(28,30)(24,26)(56,58)(60,62)(30,56)
(26,60)(58,28)(62,24) (1,43)(5,47)(37,15)(33,11)(3,13)(7, 9)(39,41)(35,45)
(17,31)(21,27)(53,59)(49,63)(19,57)(23,61)(55,29)(51,25)

(0,40)(4,44)(36,12)(32, 8)(2,14)(6,10)(38,42)(34,46)(16,28)(20,24)(52,56)(48,60)
(18,58)(22,62)(54,30)(50,26) (13,41)(9,45)(41,13)(45, 9)(15,15)(11,11)(43,43)
(47,47) (29,29)(25,25)(57,57)(61,61)(31,59)(27,63)(59,31)(63,27)(12,36)(8,32)
(40, 0)(44, 4)(14, 2)(10, 6)(42,38)(46,34)(28,16)(24,20)(56,52)(60,48)(30,54)
(26,50)(58,18)(62,22) (1,37)(5,33)(37, 1)(33, 5)(3, 3)(7, 7)(39,39)(35,35)
(17,17)(21,21)(53,53)(49,49)(19,55)(23,51)(55,19)(51,23)

(0,42)(4,46)(36,14)(32,10)(2,12)(6, 8)(38,40)(34,44)(16,30)(20,26)(52,58)(48,62)
(18,56)(22,60)(54,28)(50,24) (13,43)(9,47)(41,15)(45,11)(15,13)(11, 9)(43,41)
(47,45) (29,31)(25,27)(57,59)(61,63)(31,57)(27,61)(59,29)(63,25) (12,38)(8,34)
(40, 2)(44, 6)(14, 0)(10, 4)(42,36)(46,32)(28,18)(24,22)(56,54)(60,50)(30,52)
(26,48)(58,16)(62,20) (1,39)(5,35)(37, 3)(33, 7)(3, 1)(7, 5)(39,37)(35,33)
(17,19)(21,23)(53,55)(49,51)(19,53)(23,49)(55,17)(51,21)

(0,44)(4,12)(36, 8)(32,40)(2,24)(6,56)(38,60)(34,28)(16,10)(20,42)(52,46)(48,14)
(18,62)(22,30)(54,26)(50,58) (13,45)(9,13)(41, 9)(45,41)(15,25)(11,57)(43,61)
(47,29) (29,11)(25,43)(57,47)(61,15)(31,63)(27,31)(59,27)(63,59) (12,32)(8, 0)
(40, 4)(44,36)(14,20)(10,52)(42,48)(46,16) (28, 6)(24,38)(56,34)(60,2)(30,50)
(26,18)(58,22)(62,54) (1,33)(5, 1)(37, 5)(33,37)(3,21)(7,53)(39,49)(35,17)
(17, 7)(21,39)(53,35)(49, 3)(19,51)(23,19)(55,23)(51,55)

(0,46)(4,14)(36,10)(32,42)(2,26)(6,58)(38,62)(34,30) (16,8)(20,40)(52,44)(48,12)
(18,60)(22,28)(54,24)(50,56) (13,47)(9,15)(41,11)(45,43)(15,27)(11,59)(43,63)
(47,31) (29, 9)(25,41)(57,45)(6İ,13)(31,61)(27,29)(59,25)(63,57) (12,34)(8, 2)
(40, 6)(44,38)(14,22)(10,54)(42,50)(46,18) (28, 4)(24,36)(56,32)(60,0)(30,48)
(26,16)(58,20)(62,52) (1,35)(5, 3)(37, 7)(33,39)(3,23)(7,55)(39,51)(35,19)
(17, 5)(21,37)(53,33)(49, 1)(19,49)(23,17)(55,21)(51,53)

(0,48)(4,16)(36,20)(32,52)(2, 4)(6,36)(38,32)(34, 0)(16,22)(20,54)(52,50)(48,18)
(18,34)(22, 2)(54, 6)(50,38) (13,49)(9,17)(41,21)(45,53)(15, 5)(11,37)(43,33)
(47, 1) (29,23)(25,55)(57,51)(61,19)(31,35)(27, 3)(59, 7)(63,39) (12,60)(8,28)
(40,24)(44,56)(14, 8)(10,40)(42,44)(46,12)(28,26)(24,58)(56,62)(60,30)(30,46)
(26,14)(58,10)(62,42) (1,61)(5,29)(37,25)(33,57)(3, 9)(7,41)(39,45)(35,13)
(17,27)(21,59)(53,63)(49,31)(19,47)(23,15)(55,11)(51,43)

(0,50)(4,18)(36,22)(32,54)(2, 6)(6,38)(38,34)(34, 2)(16,20)(20,52)(52,48)(48,16)
(18,32)(22, 0)(54, 4)(50,36) (13,51)(9,19)(41,23)(45,55)(15, 7)(11,39)(43,35)
(47, 3) (29,21)(25,53)(57,49)(61,17)(31,33)(27, 1)(59, 5)(63,37) (12,62)(8,30)
(40,26)(44,58)(14,10)(10,42)(42,46)(46,14)(28,24)(24,56)(56,60)(60,28)(30,44)
(26,12)(58, 8)(62,40) (1,63)(5,31)(37,27)(33,59)(3,11)(7,43)(39,47)(35,15)
(17,25)(21,57)(53,61)(49,29)(19,45)(23,13)(55, 9)(51,41)

(0,52)(4,48)(36,16)(32,20)(2,18)(6,22)(38,54)(34,50) (16, 0)(20,4)(52,36)(48,32)
(18,38)(22,34)(54, 2)(50, 6) (13,53)(9,49)(41,17)(45,21)(15,19)(11,23)(43,55)
(47,51) (29, 1)(25, 5)(57,37)(61,33)(31,39)(27,35)(59, 3)(63, 7) (12,56)(8,60)
(40,28)(44,24)(14,30)(10,26)(42,58)(46,62) (28,12)(24,8)(56,40)(60,44)(30,42)
(26,46)(58,14)(62,10) (1,57)(5,61)(37,29)(33,25)(3,31)(7,27)(39,59)(35,63)
(17,13)(21, 9)(53,41)(49,45)(19,43)(23,47)(55,15)(51,11)

(0,54)(4,50)(36,18)(32,22)(2,16)(6,20)(38,52)(34,48) (16, 2)(20,6)(52,38)(48,34)
(18,36)(22,32)(54, 0)(50, 4) (13,55)(9,51)(41,19)(45,23)(15,17)(11,21)(43,53)
(47,49) (29, 3)(25, 7)(57,39)(61,35)(31,37)(27,33)(59, 1)(63, 5) (12,58)(8,62)
(40,30)(44,26)(14,28)(10,24)(42,56)(46,60)(28,14)(24,10)(56,42)(60,46)(30,40)
(26,44)(58,12)(62, 8) (1,59)(5,63)(37,31)(33,27)(3,29)(7,25)(39,57)(35,61)
(17,15)(21,11)(53,43)(49,47)(19,41)(23,45)(55,13)(51, 9)

(0,56)(4,60)(36,28)(32,24)(2,30)(6,26)(38,58)(34,62) (16,12)(20,8)(52,40)(48,44)
(18,42)(22,46)(54,14)(50,10) (13,57)(9,61)(41,29)(45,25)(15,31)(11,27)(43,59)
(47,63) (29,13)(25, 9)(57,41)(61,45)(31,43)(27,47)(59,15)(63,11) (12,52)(8,48)
(40,16)(44,20)(14,18)(10,22)(42,54)(46,50) (28, 0)(24,4)(56,36)(60,32)(30,38)
(26,34)(58, 2)(62, 6) (1,53)(5,49)(37,17)(33,21)(3,19)(7,23)(39,55)(35,51)
(17, 1)(21, 5)(53,37)(49,33)(19,39)(23,35)(55, 3)(51, 7)

(0,58)(4,62)(36,30)(32,26)(2,28)(6,24)(38,56)(34,60)(16,14)(20,10)(52,42)(48,46)
(18,40)(22,44)(54,12)(50, 8) (13,59)(9,63)(41,31)(45,27)(15,29)(11,25)(43,57)
(47,61) (29,15)(25,11)(57,43)(61,47)(31,41)(27,45)(59,13)(63, 9) (12,54)(8,50)
(40,18)(44,22)(14,16)(10,20)(42,52)(46,48) (28, 2)(24,6)(56,38)(60,34)(30,36)
(26,32)(58, 0)(62, 4) (1,55)(5,51)(37,19)(33,23)(3,17)(7,21)(39,53)(35,49)
(17, 3)(21, 7)(53,39)(49,35)(19,37)(23,33)(55, 1)(51, 5)

(0,60)(4,28)(36,24)(32,56)(2, 8)(6,40)(38,44)(34,12)(16,26)(20,58)(52,62)(48,30)
(18,46)(22,14)(54,10)(50,42) (13,61)(9,29)(41,25)(45,57)(15, 9)(11,41)(43,45)
(47,13) (29,27)(25,59)(57,63)(61,31)(31,47)(27,15)(59,11)(63,43) (12,48)(8,16)
(40,20)(44,52)(14, 4)(10,36)(42,32)(46, 0) (28,22)(24,54)(56,50)(60,18)(30,34)
(26, 2)(58, 6)(62,38) (1,49)(5,17)(37,21)(33,53)(3, 5)(7,37)(39,33)(35, 1)
(17,23)(21,55)(53,51)(49,19)(19,35)(23, 3)(55, 7)(51,39)

(0,62)(4,30)(36,26)(32,58)(2,10)(6,42)(38,46)(34,14)(16,24)(20,56)(52,60)(48,28)
(18,44)(22,12)(54, 8)(50,40) (13,63)(9,31)(41,27)(45,59)(15,11)(11,43)(43,47)
(47,15) (29,25)(25,57)(57,61)(61,29)(31,45)(27,13)(59, 9)(63,41) (12,50)(8,18)
(40,22)(44,54)(14, 6)(10,38)(42,34)(46, 2) (28,20)(24,52)(56,48)(60,16)(30,32)
(26, 0)(58, 4)(62,36) (1,51)(5,19)(37,23)(33,55)(3, 7)(7,39)(39,35)(35, 3)
(17,21)(21,53)(53,49)(49,17)(19,33)(23, 1)(55, 5)(51,37)

Figure A.2- Partitioning for 64-QAM

APPENDIX B - OPTIMUM ROTATION ANGLE FOR COMPONENT DIVERSITY

Component diversity requires that each symbol in a signal set possess unique components. Furthermore, the product of the difference between two symbol components should be maximized. Each signal set should be rotated by an angle θ in order to satisfy the above conditions. This appendix develops a general expression for the angle θ in term of the symbol components for the two dimensional case. The optimum rotation angle for 8-SQ and 16-QAM is then derived.

Let $a_0 \ldots a_M$ be M symbols in a signal set. Let $b_0 \ldots b_M$ be the symbols rotated clockwize by the optimum angle θ. The components of a symbol b_i in terms of the components of a symbol a_i are given by:

$$\begin{bmatrix} b_{ix} \\ b_{iy} \end{bmatrix} = \begin{bmatrix} \cos\theta & -\sin\theta \\ \sin\theta & \cos\theta \end{bmatrix} \begin{bmatrix} a_{ix} \\ a_{iy} \end{bmatrix} = \begin{bmatrix} a_{ix}\cos\theta - a_{iy}\sin\theta \\ a_{ix}\sin\theta + a_{iy}\cos\theta \end{bmatrix}$$

Let d_{uv}^2 represent the product of the square of the difference between the components of two symbols u and v. Then

$$d_{uv}^2 = (b_{ux} - b_{vx})^2 (b_{uy} - b_{vy})^2$$

$$= [(a_{ux}\cos\theta - a_{uy}\sin\theta) - (a_{vx}\cos\theta - a_{vy}\sin\theta)]^2 [(a_{ux}\sin\theta + a_{uy}\cos\theta) - (a_{vx}\sin\theta + a_{vy}\cos\theta)$$

$$= [(a_{ux} - a_{vx})\cos\theta - (a_{uy} - a_{vy})\sin\theta]^2 [(a_{ux} - a_{vx})\sin\theta + (a_{uy} - a_{vy})\cos\theta]^2$$

Let $\alpha = a_{ux} - a_{vx}$ and $\beta = a_{uy} - a_{vy}$, then

$$d_{uv}^2 = [\alpha\cos\theta - \beta\sin\theta]^2 [\alpha\sin\theta + \beta\cos\theta]^2 .$$

Expanding and grouping the terms results in

$$d_{uv}^2 = \left(\alpha^2\beta^2\cos^4\theta - 2\alpha^2\beta^2\cos^2\theta\sin^2\theta + \alpha^2\beta^2\sin^4\theta\right) + (\alpha^4 + \beta^4 - 2\alpha^2\beta^2)\cos^2\theta\sin^2\theta$$
$$+(2\alpha^3\beta - 2\alpha\beta^3)\sin\theta\cos\theta\left(\cos^2\theta - \sin^2\theta\right)$$

$$= \left(\alpha\beta\cos 2\theta + \left(\frac{\alpha^2 - \beta^2}{2}\right)\sin 2\theta\right)^2$$

To find the optimum rotation angle, this expression is differentiated with respect to θ and set equal to zero. This yields

$$\left(\frac{\alpha^4 + \beta^4 - 6\alpha^2\beta^2}{8}\right)\sin 4\theta + \left(\frac{\alpha^3\beta - \alpha\beta^3}{2}\right)\cos 4\theta = 0 \qquad (B-1)$$

This expression is now applied to 8-SQ and 16-QAM signal constellations. First, consider the 8-SQ signal set shown in Figure B.1. The symbols that are closest together are of most interest because the product of the difference between their components will be the smallest. Furthermore, there is some symmetry in the signal set. Therefore, only the pairs of symbols 3,5 and 3,2 need to be considered.

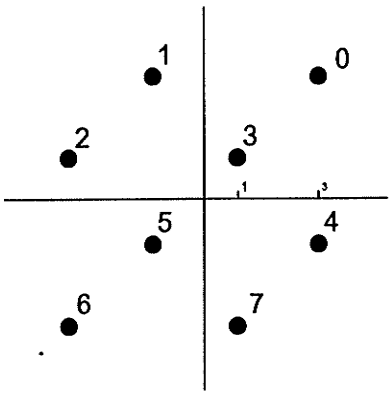

Figure B.1 - 8-SQ signal set

For the pair of symbols 3 and 5, $\alpha = 1 - (-1) = 2$ and $\beta = 2$. Entering these values in equation (B-1) and simplifying yields

$$\sin 4\theta = 0$$

$$\text{or } \theta = (2n+1)\frac{\pi}{8}$$

For the pair of symbols 3 and 2, $\alpha = 4$ and $\beta = 0$. Substituting these values in equation B-1, yields $\sin 4\theta = 0$. Therefore, the optimal angle to rotate the signal set to maximize d_{uv}^2 is $\pi/8$. By finding the new co-ordinates of the rotated signal set, it is simple to verify that all symbols differ in both components.

Now, consider the 16-QAM signal set shown at Figure B.2. Again, the objective is to maximize d_{uv}^2 for the symbols closest together. Because of the symmetry of the signal set, only the pairs of symbols 6,5 and 6,10 need to be considered. The case for the pair of symbols 6,10 is identical to the pair of symbols 3,2 for 8-SQ. For the pair of symbols 6 and 5, $\alpha = 1-(-1) = 2$ and $\beta = 0$. Substituting these values in equation B-1 yields an optimal rotation angle of $\theta = \pi/8$ as above.

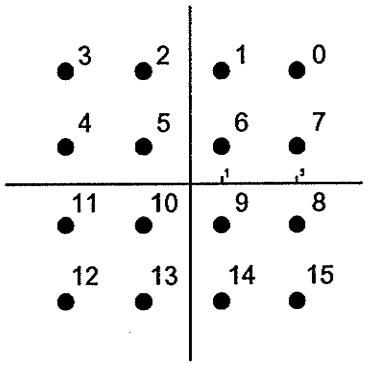

Figure B.2 - 16-QAM signal set